HYGRO-THERMO-MECHANICALLY INDUCED NONLINEAR TRANSVERSE CENTRAL DEFLECTION ANALYSIS OF PIEZOELECTRIC ELASTICALLY SUPPORTED LAMINATED COMPOSITE SANDWICH PLATE WITH SYSTEM RANDOMNESS USING SECANT FUNCTION BASED SHEAR DEFORMATION THEORY

[1]Mr. Nikhil M Kulkarni, [2]Dr. Achchhe Lal
[1]Assistant Professor, [2]Associate Professor
[1]Mechanical Engineering Department,
[1] PIET, Parul University, Vadodara, India

Abstract : In the present manuscript statistics of transverse nonlinear central deflection of elastically supported piezoelectric laminated composite sandwich plate (ESPLCSP) subjected to hygro-thermo-mechanical loading using micromechanical approach is evaluated. System randomness as micro-level material properties of fiber and matrix, material properties of piezoelectric, laminate thickness, lamination angle, foundation parameters, and load intensity are taken as independent random variables. The mechanical loading is taken as uniformly distributed and sinusoidal loadings. The secant function based shear deformation theory (SFSDT) with von-Karman nonlinearity is used for basic formulation. The elastic and hygrothermal properties of the composite material are considered to be dependent on temperature and moisture concentration have been evaluated utilized micromechanical modeling. A Newton-Raphson method based on C0 nonlinear finite element method combined with mean centered second order perturbation technique (SOPT) proposed by present authors for the composite plate is extended for sandwich composite plate. The effect of random system properties with changing the plate geometry, stacking sequences, support conditions, foundation parameters, piezoelectric layers, fiber volume fraction and temperature, and moisture distribution on ESPLCSP is presented. The performance of proposed approach is validated through comparison with those available in the literatures and independent Monte Carlo simulation (MCS).

Keywords: **Laminated composite sandwich plate, Nonlinear bending response, Random system properties, Elastic foundation, SOPT, secant function based shear deformation theory**

1. INTRODUCTION

The laminates composite sandwich plates in which inner layers are replaced by a core with low stiffness are used to resist in-plane and lateral loads while the core material resists transverse shear loads. These materials are being increasingly used in aerospace, aeronautical and others modern applications due to high specific modulus and strength, low specific density, high structural efficiency and durability with improved fatigue and impact resistance.

To use them efficiently, it is necessary to develop appropriate model for accurately predicting their structural behaviour in terms of linear and/or nonlinear bending and stress distribution.

These laminated composite structures are often subjected to hygrothermomechanical loadings simultaneously or separately under severe environmental conditions during their operational life. The hygrothermal loadings arise due to increased temperature and absorbed moisture concentration may cause degradation in strength and stiffness of the structures, and ultimately deteriorating the performance of the structures. Aside from this, structures are often subjected to high intensity of mechanical loads in terms of sinusoidal and uniform distributed loadings (UDL) that may change the results in linear or nonlinear load deflection curve. Due to lower strength of laminated composite in transverse directions compared to isotropic materials, knowledge pertaining to transverse deformation is extremely important for optimum and safe design of the structures.

The micromechanical approach is amongst very popular approach to evaluate the equivalent material properties composite material from known constituents' material properties of matrix and fibre based on their relative volume. It is because of equivalent material properties of composite are not known at different ply levels. The main purpose objective of micromechanical approach is tailoring the mechanical properties in terms of strength and stiffness in particular positions and directions as per requirements.

In the current scenario, structures should be self-monitoring and self controlling capabilities under the influence of external stimuli. This can be achieved by inserting piezoelectric layer as smart layer at different positions of fibre layers. Hence, effect of piezoelectric layer at different positions of fibre layers is the one of interesting topic for researchers.

Any kind of structure is often subjected to elastic foundation to observe shocks and vibrations and provides stability to the structures. This objective can be achieved by attaching two parameters Pasternak elastic foundation, It is because of this type of

foundation prevent both transverse and lateral deformation and most appropriate for design prospective. Therefore, proper examination of elastic foundation on the performance of structure is needed.

During manufacturing and processing, composite materials pose large number of randomness in material, geometrical and external loading which affected the overall response and ultimately affect the final design. For factor of safety point of view, the individual or combined effect of randomness on structural response is very interesting topic to the researchers.

Hence there is a need to study deflection behaviour of laminated composite sandwich plate with system randomness using probabilistic approach. Probabilistic approach provides a tool to quantify system uncertainties in the structural responses in terms of mean and variance. Large numbers of literatures are available on the linear and nonlinear static response of sandwich structures with various shear deformation theory subjected to hygro-thermo-mechanical loadings acting simultaneously or combined using deterministic approach.

A considerable volume of literatures is available on the linear and nonlinear bending response of composite laminated plates/shells based on deterministic approach under various thermal and/or mechanical loads and/or combination of these. Among them are Reddy [1], Reddy and Chao [2], Zenkour [3], Houliara and Karamanos [4], Chan and Chung [5], Huang and Tauchert [6] and [7], Chandrasekhara and Bhimaraddi [8] and Reddy and Chandrasekhara [9]. Very little number of literatures are available for static response of laminated composite plate based on micro-mechanical approach (See for examples [Ram and Sinha [10], Shen [11] and Upadhyay et al. [12]). All the literatures mentioned above are based on the assumptions of the complete determinacy of the structural parameters which gives only mean response and unaccounted the randomness caused by inherent random system parameters.

Literatures available for analysis of composite structures with random system properties are limited. Zongeen and Suhaun [13] presented a method to estimate the standard deviation of eigenvalue and eigenvector of random multiple degree of freedom (MODF) system. Naveenth Raj et al. [14] have evaluated the linear static response statistics of graphite-epoxy composite laminates with randomness in material properties for different boundary conditions, thickness ratios, aspect ratios and fibre orientations to deterministic loading by using combination of finite element analysis (FEM) and Monte Carlo simulation (MCS). Salim et al. [15] examined the effect of randomness in material properties on the response statistics of a composite plate subjected to static loading using classical plate theory (CLT) in conjunction with first order perturbation techniques (FOPT). Onkar and Yadav [16] investigated the non-linear response statistics of composite laminated plate with random material properties subjected to transverse random loading based on CLT in conjunction with FOPT. Yang et al. [17] have investigated the stochastic bending response of moderately thick compositionally graded plates with random thermo-mechanical properties under lateral load and uniform temperature change. They have utilized a first order perturbation technique (FOPT) to obtain the response statistics, while basic formulation of the problem has been developed based on Reddy's higher order shear deformation theory (HSDT). Falsone and Impollonia [18] proposed a method for evaluating the static response of structures with uncertain material properties providing results with good level of accuracy, even for high amount of uncertainties. Zhang et al. [19] evaluated the response and reliability of the uncertain structures using the stochastic perturbation method to vector-valued and matrix-valued function. Liu et al. [20] formulated the probabilistic finite element method (PFEM) for linear and nonlinear continua with homogeneous random fields of a one-dimensional elastic plastic wave propagation problems and a two-dimensional plane-stress beam bending problem. Zhang and Ellingwood [21] examined the effect of random material field characteristics on the instability of a simply supported beam on elastic foundation and a frame using perturbation technique. Noh [22] investigated the effect of multiple uncertain material properties on the response variability of in-plane and plate structures with multiple uncertain material parameters using stochastic finite element analysis to. In order to incorporate the uncertainties of the physical properties of laminated composite structures, a stochastic finite element–based second moment was developed by Park et al. [23]. Lal et al., [24,25] and Singh et al., [26] have presented C^0 linear and nonlinear finite element method (FEM) in conjunction with a mean centred FOPT to obtain the second order response statistics of linear and nonlinear bending response of laminated composite plate resting on elastic foundation subjected to thermal and/or lateral loading . Pandit et al. [27] investigated the statistics of deflection of sandwich plate under transverse mechanical loading using the improved layer-wise plate theory and C^0 stochastic finite element method (SFEM).

To the best of the authors· knowledge, there is no literature covering the second order statistics of nonlinear transverse central response of laminated composite piezoelectric elastically supported laminated composite sandwich plate with system randomness subjected to hygro-thermo-mechanical loadings using micromechanical approach through Newton-Raphson method. This is the problems studied in the present paper.

The mean cantered second order perturbation method (SOPT) using C° nonlinear finite element method through secant function based shear deformation theory (SFSDT) is employed to determine the mean and coefficient of variation of nonlinear transverse central deflection of laminated composite piezoelectric elastically supported sandwich plate with temperature and moisture dependent material properties subjected to uniform constant temperature and moisture concentration. The effect of volume fractions of fibres, plate thickness and aspect ratios, load parameters, lamination angle, position of piezoelectric layers, foundation parameters, boundary conditions, and temperature and moisture contents with random system properties on mean and COV of transverse central deflection response subjected to UDL and sinusoidal loadings are investigated

2. FORMULATION

2.1 GEOMETRY OF PIEZOLAMINATED ELASTICALLY SUPPORTED PLATE

The piezoelectric multilayered composite plate resting on elastic foundation having length *a*, width *b*, thickness *h* located in the three dimensional Cartesian coordinate system (x, y, z) is shown in Fig.1. Where (x, y, z) are the axial, tangential, and normal to the mid plane of the plate respectively. The assumption of perfect bonding exists between fibre and matrix and their effect will be considered as separately. The piezoelectric layer is attached at different positions of fibre layers with neglected thickness. Plate is supported by most efficient two parameters Pasternak elastic foundation with spring and shear layers by elastic foundations as K_1 and K_2, respectively. Without assuming any separation between plate and supporting foundation, the reaction force (P) per unit area can be written as [11-12]

$$P = K_1 w - K_2 \left[\frac{\partial^2 w}{\partial x^2} + \frac{\partial^2 w}{\partial y^2} \right] \tag{1}$$

In Eq. (1), when shear neglected, the plate will become Winkler foundation model.

2.2 Displacement model

The displacement field model is based on recently developed secant function based shear deformation theory (SFSDT) given by Grovar et al. [35]. The proposed theory involve non-linear shear stress distribution which satisfies the zero transverse shear conditions on top and bottom surfaces as a priori and therefore a shear correction factor is not required.

The main purpose to use SFSDT is to increase the computational accuracy and time at each ply level as compared to higher order shear deformation theory (HSDT). In HSDT, number of unknown variables are higher, therefore, computation computational time for evaluation of these variables are higher. The SFSDT is based on Taylor series expansion and expansion order can be extended more than third order. The constants involved in SFSDT are computed easily as compared to HDST. Hence, computational response using SFSDT is more accurate as compared to HSDT.

The Displacement fields ($\bar{u}$, $\bar{v}$, $\bar{w}$) at any point along (x, y, z) directions for a composite plate can be expressed as

$$\begin{aligned} \bar{u}(x,y,z) &= u(x,y) - z\frac{\partial w}{\partial x} + \left(g(z) + z\Omega\right)\theta_x(x,y) \\ \bar{v}(x,y,z) &= v(x,y) - z\frac{\partial w}{\partial y} + \left(g(z) + z\Omega\right)\theta_y(x,y) \\ \bar{w}(x,y,z) &= w(x,y) \end{aligned} \tag{2}$$

$$\text{where } g(z) = z\,sec\left(\frac{rz}{h}\right) \text{ and } \Omega = -\frac{sec\left(\frac{r}{2}\right)}{\left(1 + \frac{r}{2}tan\left(\frac{r}{2}\right)\right)} \tag{3}$$

The parameter *r* is the transverse shear stress parameter and its value is ascertained by the inverse method in post processing step 0.1. The parameters Ω is a constant and is evaluated by implementing the transverse shear stress boundary conditions so that the transverse shear stresses at the boundary vanish. g(z) is the shear strain functions used in the SFSDT.

The displacement field model in Eq. (2), C^1 continuity occurs in the structural kinematics. The solution of finite element problem using C^1 continuity requires more computational cost and extra complexity. The C^1 continuity problem may be reduces to C^0 continuity by including two additional independent field variables as $\varphi_x = \partial w/\partial x$ and $\varphi_y = \partial w/\partial y$ in Eq. (2). These two additional independent field variables causes' additional constraints are satisfied by employing the penalty parameter. This is circumvented by expressing the displacement field in the following form [21-22, 31-34]

$$\begin{aligned} \bar{u} &= u - z\varphi(x) + \left(g(z) + z\Omega\right)\theta_x \\ \bar{v} &= v - z\varphi(x) + \left(g(z) + z\Omega\right)\theta_y \\ \bar{w} &= w \end{aligned} \tag{4}$$

The displacement field vector {*q*} is expressed as

$$q = \begin{pmatrix} u & v & w & \theta_2 & \theta_1 & \varphi_2 & \varphi_1 \end{pmatrix}^T \tag{5}$$

2.3 Strain displacement relations

The strain-displacement relations are obtained by using large deformation theory with von-Karman nonlinearity. The total strain vectors associated with displacement for lamina layers can be expressed as

$$\{\varepsilon\} = \{\varepsilon_l\} + \{\varepsilon_{nl}\} - \{\varepsilon_p\} \tag{6}$$

The linear strain tensor $\{\varepsilon_l\}$ based on HSDT can be written as

$$\{\varepsilon_l\} = [T]\{\bar{\varepsilon}_l\} \tag{7}$$

where, *T* is the function of Z and unit step vector defined in appendix A.1 and $\{\bar{\varepsilon}_l\}$ is reference plain linear strain tensor defined as

$$\{\bar{\varepsilon}_l\} = \left\{\varepsilon_1^0 \quad \varepsilon_2^0 \quad \varepsilon_6^0 \quad k_1^0 \quad k_2^0 \quad k_6^0 \quad k_1^2 \quad k_2^2 \quad k_6^2 \quad \varepsilon_4^0 \quad \varepsilon_5^0 \quad k_4^2 \quad k_5^2\right\}^T \tag{8}$$

From Eq. (5), Eq. (8) can be written as

$$\{\bar{\varepsilon}_l\} = [L]\{q\} \tag{8a}$$

Where L is the strain displacement matrix and defined in Appendix A.2.

The nonlinear strain vector $\{\varepsilon_{nl}\}$ in von-Karman sense can be written as [31-34]

$$\{\varepsilon_{nl}\} = \frac{1}{2}[A]\{\phi\} \tag{9}$$

Where

$$[A] = \frac{1}{2}\begin{bmatrix} w_{,x} & 0 & w_{,y} & 0 & 0 \\ 0 & w_{,x} & w_{,y} & 0 & 0 \end{bmatrix}^T \tag{10}$$

and $$\phi = \frac{1}{2}\begin{bmatrix} w_{,x} \\ w_{,y} \end{bmatrix} \tag{11}$$

here (,) denotes partial differential.

The piezoelectric strain vector $\{\bar{\varepsilon}^P\}$ can be represented as

$$\{E\} = \{E_x \quad E_y \quad E_z\} = [T_\phi]\{E^{(0)}\} \tag{12}$$

Where $[T_\Phi]$ and $[E]$ is the electric field potential operator and electric field vector, respectively and defined in Appendix A. 3.

2.4 Micromechanical approach

The effective materials properties of the fibre reinforce composite at given temperature can be evaluated using micromechanical model proposed by Chamis and Sinclair (1982). Since, the effect of induced temperature is dominant in matrix material. Hence the degradation of the fibre reinforced composite material properties is estimated by degrading the matrix property only. The matrix mechanical property retention ratio can be expressed as Chamis and Sinclair (1982).

$$F_m = \left[\frac{T_{gw} - T}{T_{g0} - T_0}\right]^{\frac{1}{2}} \tag{13}$$

where T=To+ ΔT and T is the temperature at which material property is to be predicted; The parameters T_{gw} and T_{go} are glass transition temperature for wet and reference dry conditions, respectively. The glass transition temperature for wet material can be determined as (23-27)

$$T_{gw} = \left(0.005C^2 - 0.10C + 1.0\right)T_{g0} \tag{14}$$

where C=Co+ ΔC and C is the moisture weight at which properties is to be evaluated. For the generated results the values of T_0 and C_0 are taken as 21^0C and C_0=0%.

The elastic constants using micromechanical approach are obtained from the following equations as written as (25, 27, 38-39)

$$E_{11} = E_{f1}V_f + F_m E_m V_m \tag{15}$$

$$E_{22} = \left(1 - \sqrt{V_f}\right)F_m E_m + \frac{F_m E_m \sqrt{V_f}}{1 - \sqrt{V_f}\left(1 - \frac{F_m E_m}{E_{f2}}\right)} \tag{16}$$

$$G_{12} = \left(1 - \sqrt{V_f}\right)F_m G_m + \frac{F_m G_m \sqrt{V_f}}{1 - \sqrt{V_f}\left(1 - \frac{F_m G_m}{G_{f12}}\right)} \tag{17}$$

$$\nu_{12} = \nu_{f12}V_f + \nu_m V_m \tag{18a}$$

$$G_m = \tag{18b}$$

Where "V" is the volume fraction and subscripts "f" and "m" are used for fibre and matrix, respectively. The effect of increased temperature and moisture concentration on the coefficients of thermal expansion (α) and moisture concentration (β) are opposite from the corresponding effect on strength and stiffness. The matrix thermal property retention ratio is approximated as

$$F_h = \frac{1}{F_m} \tag{18c}$$

2.5 Constitutive equation

The constitutive law of thermo-piezo-elastic constitutive relationship for material under consideration relates the stresses with strains in plan-stress state for the kth orthotropic lamina is given as [33]

$$[\sigma] = [Q]\{\varepsilon\} - [e]\{E\} \tag{19}$$

Where [Q] is the constitutive elastic stiffness matrix defined in Appendix A.4

Where [e] is defined as piezoelectric constant and expressed by

$$[e] = \begin{bmatrix} 0 & 0 & 0 & e_{14} & e_{15} \\ 0 & 0 & 0 & e_{24} & e_{25} \\ e_{31} & e_{32} & e_{36} & 0 & 0 \end{bmatrix}^T \tag{20}$$

Here [E] is the electric field vector defined by

$$\{E\} = \begin{bmatrix} E_x & E_y & E_z \end{bmatrix}^T = \begin{bmatrix} -\frac{\partial \phi}{\partial x} & -\frac{\partial \phi}{\partial y} & -\frac{\partial \phi}{\partial z} \end{bmatrix}^T \tag{21}$$

Where ϕ is electric potential and defined in Appendix A-5.

2.6 Strain energy of the piezolaminated composite plates

The elastic strain energy of a piezoelectric laminated composite plate is expressed as

$$U=\frac{1}{2}\int_V \{\varepsilon\}^T \{\sigma\}\, dV-\frac{1}{2}\int_V \{E\}^T \{D\}\, dV \tag{22}$$

The parameter [D] is the electric field displacement and defined as the elastic strain energy becomes

$$\{D\}=[e]^T \{\varepsilon\}+[k]\{E\} \tag{23}$$

Where [*k*] is the dielectric constant matrix and defined in appendix A.6.
Substituting Eq. (19), (23) and (39) in Eq. (22), Eq. (22) becomes

$$U=\frac{1}{2}\int_v \left(\varepsilon^T\left[\overline{Q}\varepsilon-eE\right]-E^T\left[e^T\varepsilon+kE\right]\right)dV. \tag{24}$$

Substituting Eq. (8) in Eq. (24) once can be written as

$$U=\frac{1}{2}\int_v \left((\varepsilon_l+\varepsilon_{nl})^T\left[\overline{Q}(\varepsilon_l+\varepsilon_{nl})-eE\right]-E^T\left[e^T(\varepsilon_l+\varepsilon_{nl})+kE\right]\right)dV \tag{25}$$

Using Eq. (25), linear potential energy can be written as

$$U_l=\frac{1}{2}\int_v \left(\varepsilon_l{}^T\left[\overline{Q}\varepsilon_l-eE\right]-E^T\left[e^T\varepsilon_l+kE\right]\right)dV \tag{26}$$

Substituting Eq. (8a) and (11) in Eq. (26), Eq. (26) can be rewritten as

$$U_L=\frac{1}{2}\int_A \left(q^T L^T DLq-q^T L^T D_1 L_\phi \phi-\phi^T L_\phi{}^T D_1^T Lq-\phi^T L_\phi{}^T D_2 L_\phi \phi\right)dA \tag{27}$$

Where D, D_1 and D_2, are the elastic stiffness matrix of composite and piezoelectric material, respectively and defined in Appendix **A. 7(a-c)**.
Using Eq. (25), after substituting Eq. (8a) and (9), the nonlinear potential energy of piezoelectric composite plate is written as

$$U_{nl}=\frac{1}{2}\int_A \left(q^T L^T D_3 A\phi+A^T\phi^T D_4 qL+A^T\phi^T D_5 A\phi-A^T\phi^T D_6 L_\varphi \varphi-L_\varphi^T\varphi_\varphi^T D_7 A\phi\right)dA \tag{28}$$

Where [D_3], [D_4], [D_5] are the nonlinear elastic matrix and [D_6], and [D_7] are the piezoelectric stiffness matrix, respectively and defined in Appendix A.8.

2.7 Strain energy due to elastic foundation

Using Eq. (1), the strain energy due to elastic foundation using two parameter Pasternak elastic foundation having shear deformable layer can be written as [31-3]

$$U_f=\frac{1}{2}\int_A\left[K_1(w)^2+K_2\left\{(w_{,x})^2+(w_{,y})^2\right\}\right]dA=\frac{1}{2}\int_A\begin{Bmatrix} w \\ w_{,x} \\ w_{,y}\end{Bmatrix}^T\begin{bmatrix} K_1 & 0 & 0 \\ 0 & K_2 & 0 \\ 0 & 0 & K_2\end{bmatrix}\begin{Bmatrix} w \\ w_{,x} \\ w_{,y}\end{Bmatrix}dA \tag{29}$$

Eq. (29) can be rewritten as

$$U_f=\frac{1}{2}\int_A \frac{1}{2}\varepsilon_f^T D_f \varepsilon_f\, dA \tag{30}$$

Where $\varepsilon_f=L_f w$ with $L_f=\begin{bmatrix}0&0&1&0&0&0&0\\0&0&\partial_{,x}&0&0&0&0\\0&0&\partial_{,y}&0&0&0&0\end{bmatrix}$ and $D_f=\begin{bmatrix}K_1&0&0\\0&K_2&0\\0&0&K_2\end{bmatrix}$

2.8 Potential due to external mechanical loading

The potential due to external work done by external mechanical load $q_{SL}(x,y)$ is given by

$$V=-W_M=\int_A q_{SL}(x,y)\; w\, dA \tag{31}$$

where, q_{SL}(x, y) is the intensity of distributed transverse and sinusoidal static load which are defined as

$$q_{SL}(x,y)=\frac{QE_{22}h^3}{b^4} \quad \text{and} \quad q_{SL}(x,y)=q0\sin\left(\frac{\pi x}{a}\right)\sin\left(\frac{\pi y}{b}\right) \tag{32}$$

here *Q* and q_0 are represented as uniform lateral pressure and sinusoidal load respectively.

2.9 Finite element model

In general, a closed form solution is difficult to obtain for buckling problems for complex boundary conditions and shapes. Therefore, FEM is the one of powerful tool used for finding an approximate solution of the problem. The displacement field vector can be written in terms of shape functions as [31-34]

Displacement vector $\{q\}$ in equation (5) and Eq (21) can be written in terms of shape functions as

$$\{q\}=\sum_{i=1}^{NN}[N_i]\{q_i\}, \qquad \text{and} \quad \{\phi\}=\sum_{i=1}^{NN}[N_{\phi i}]\{\phi_i\}, \tag{33}$$

here *i* represent node number and N_i is shape function at i^{th} node.

For an element, displacement field vector, and electric potential vector can be written as

$$\{q\}^{(e)} = [N_i]^{(e)} \{q\}^{(e)} \text{ and } \{\phi\}^{(e)} = [N_\phi]^{(e)} \{q_\phi\}^{(e)} \tag{34}$$

Substituting Eq. (34) in Eq. (27), and summed over all elements using finite element model Eq. (33), Eq (27) linear strain energy of the piezolaminated plate can be rewritten as

$$U_l^{(e)} = \sum_{i=1}^{NE} \left(q^{(e)T} K^{(e)} q^{(e)} - q^{(e)T} K_1^{(e)} q_\phi^{(e)} - q_\phi^{(e)T} K_1^{(e)T} q^{(e)} - q_\phi^{(e)T} K_2^{(e)} q_\phi^{(e)} - q^{(e)T} F_t^{(e)} \right)$$

(35)

Where

$$K^{(e)} = \frac{1}{2} \int_{A^{(e)}} B^{(e)T} D B^{(e)} dA,\ K_1^{(e)} = \frac{1}{2} \int_{A^{(e)}} B^{(e)T} D_1 B_\phi^{(e)} dA, \text{ and } K_2^{(e)} = \frac{1}{2} \int_{A^{(e)}} B_\phi^{(e)T} D_2 B_\phi^{(e)} dA, \tag{36}$$

Here $K^{(e)}$, $K_1^{(e)}$ and $K_2^{(e)}$ are the element bending stiffness matrix, coupling matrix and dielectric matrix, respectively. The strain displacement matrix [B] for plate and piezoelectric [B_g] can be written as

$$[B]^{(e)} = [L][N_i]^{(e)}, \text{ and } [B_\phi]^{(e)} = [L_\phi][N_\phi]^{(e)}. \tag{37}$$

$$\text{with } [B]^{(e)} = [B_1 \quad B_2 \quad B_3 \quad \cdot \quad \cdot \quad \cdot \quad B_{NN}] \text{ and } [B_i] = [L]N_i. \quad i=1, 2, 3,\ldots\ldots NN \tag{38}$$

Similarly, using Eq. (28) and Eq. (33), the nonlinear strain energy for piezolaminated plate after summing over the entire element using finite element analysis can be rewritten as

$$U_{nl}^{(e)} = \sum_{i=1}^{NE} \begin{pmatrix} \{q^{(e)}\}^T k_1^{(e)} \{q^{(e)}\} + \{q^{(e)}\}^T k_2^{(e)} \{q^{(e)}\} + q^{(e)}\}^T k_3^{(e)} \{q^{(e)}\} \\ -\{q^{(e)}\}^T k_4^{(e)} \{q_\phi^{(e)}\} - \{q_\phi^{(e)}\}^T k_5^{(e)} \{q^{(e)}\} \end{pmatrix} \tag{39}$$

where $k_1^{(e)} = \frac{1}{2} \int_{A^e} B^{(e)T} D_3 \{A^{(e)}\} \{G^{(e)}\} dxdy$, $k_2^{(e)} = \frac{1}{2} \int_{A^e} \{G^{(e)}\}^T \{A^e\}^T D_4 \{B^{(\varepsilon)}\} dxdy$ and

$k_3^{(e)} = \frac{1}{2} \int_{A^e} \{G^{(e)}\}^T \{A^{(e)}\}^T D_5 \{A^{(e)}\} \{G^{(e)}\} dxdy$ are the element bending stiffness matrix and

$k_4^{(e)} = \frac{1}{2} \int_{A^e} \{G^{(e)}\}^T \{A^{(e)}\}^T D_6 \{B_\phi\} dxdy$ and $k_5^{(e)} = \frac{1}{2} \int_{A^e} \{B_\phi^{(e)}\}^T D_7 \{A^{(e)}\} \{G^{(e)}\} dxdy$

are the coupling matrix, respectively.

Similarly, strain energy due to foundation after summing over all the element using Eq. (33), Eq. (30) can be rewritten as

$$U_f^{(e)} = \sum_{i=1}^{NE} \left\{ q^{(e)} \right\}^T K_f^{(e)} \left\{ q^{(e)} \right\} \tag{40}$$

where $K_f^{(e)} = \frac{1}{2} \int_{A^{(e)}} B_f^{(e)T} D_f B_f^{(e)} dA$, is the foundation stiffness matrix and [B_f] is the strain displacement matrix due to foundation and defined as

$$\left[B_f \right]^{(e)} = \left[L_f \right] [N]^{(e)} \tag{41}$$

Using finite element model as Eq. (33), potential of work done due to mechanical loading as given Eq. (31) can also be written as

$$V = \sum_{e=1}^{NE} V^{(e)} = \{q\}^T F \tag{42}$$

Where

$$F = \begin{pmatrix} 0 & 0 & q_{SL} & 0 & 0 & 0 & 0 \end{pmatrix}^T$$

Adopting numerical integration, the element bending stiffness matrix consist of linear and nonlinear, coupling matrix, dielectric stiffness matrix, foundation stiffness matrix and geometric stiffness matrix can be obtain by transforming expression in (x, y) coordinate system to natural coordinate system (ξ, η) using Gauss quadrature.

3. Governing equation

The governing equation for the nonlinear bending analysis can be derived using Variational principle, which is generalization of the principle of virtual displacement [30, 31]. For the bending analysis, the minimization of first variation of total potential energy (Π) with respect to displacement vector must be zero.

$$\frac{\partial \prod}{\partial q^T} = 0 \tag{43}$$

The total potential energy $\prod$ can be expressed as

$$\prod = U_l + U_{nl} + U_f + V \tag{44}$$

Substituting Eq. (35), Eq. (39), Eq.(40) and Eq.(42) in Eq. (44), Eq. (44) can be rewritten as

$$\left[K^* \right] \{q\} = \{F\} \tag{45}$$

where $K^* = K_q - K_{q\_phi} K_{phi}^{-1} K_{q\_phi}^T + K_f$ (46)

here $K_q = \sum_{e=1}^{NE}(K^{(e)} + K_1^{(e)} + K_2^{(e)})$, $K_{q\_phi} = \sum_{e=1}^{NE}(K1^{(e)} + K_4^{(e)})$, $K_{phi} = \sum_{e=1}^{NE} K_2^{(e)}$, $F = \sum_{e=1}^{NE} F^{(e)}$ and $K_f = \sum_{e=1}^{NE} K_f^{(e)}$

The parameters K_q, K_{q_phi}, K_1^T, K_{phi} and *F* are the global elastic stiffness matrix, coupling matrix between elastic mechanical and electrical effect, dielectric stiffness matrix, force vector and foundation stiffness matrix, respectively.

4. Solution Approach

Solution approach -A Newton Raphson method

The nonlinear differential equation (45) can be reduced to set of nonlinear equation as

$$K^*\left(\{q\}\right)\{q\} = \{F^*\} \qquad (47)$$

In order to solve solve the Eq. (47), the Newton–Raphson method is used for the solution of nonlinear governing equations. The residue can be written as (Simsek and Kocaturk (2009), Reddy (2004) , William et al. (1992))

$$R\{q\} = K^*\left(\{q\}\right)\{q\} - \{F^*\} = 0 \qquad (48)$$

By assuming that the solution $\{q\}^{(i-1)}$ at the (*i*-1) iteration is known, the residual vector R can be expanded using Taylor's series about the solution $\{q\}^{(i-1)}$ as follows:

$$R\left(\{q\}\right) = R\left(\{q\}^{(i-1)}\right) + \left(\frac{\partial R\left(\{q\}\right)}{\partial\{q\}}\right)^{(i-1)} .\delta\{q\} + \ldots = 0 \qquad (49)$$

Neglecting the terms of order two and higher gives the following equations:

$$K_T^*\left(\{q\}^{i-1}\right)\delta\{q\} = -R\left(\{q\}^{(i-1)}\right) = \{F^*\} - K^*\left(\{q\}^{i-1}\right)\{q\}^{i-1} \qquad (50)$$

Where K_T^* is the tangent stiffness matrix and can be written as

$$\left[K_T\left(\{q\}^{(i-1)}\right)\right] = \left(\frac{\partial R\left(\{q\}\right)}{\partial\{q\}}\right)^{(i-1)} \qquad (51)$$

Incremental displacements $\delta\{q\}$, the displacement vector $\{q\}^i$ for *i*th iteration can be written as

$$\{q\}^i = \{q\}^{(i-1)} - \left[K_T^*\{q\}^{(i-1)}\right]^{-1} R\left(\{q\}^{(i-1)}\right) \qquad (52)$$

This procedure is continued until the difference between two successive solution vectors is less than a selected tolerance criterion. Once Eq. (55) is solved for the displacements {*q*} at time *t*+Δ*t*, the new acceleration vector $\ddot{q}$, and the new velocity vector $\dot{q}$ at time *t*+Δ*t* are computed from the Eq. (45) and Eq. (46). For solving the nonlinear equations, the initial solution vector is chosen to be zero vector, namely, the first iteration solution corresponds to the linear solution.

4.2 Solution approach: perturbation technique

The governing equation (23) can be written in the most general form as:

$$\left[K_{ij}^R\right]\left\{q_j^R\right\} = \left\{F_i^{(R)}\right\} \qquad (24)$$

where $\left[K^R\right]$, $\left[q_j^R\right]$ and $\left\{F_i^R\right\}$ are represented as the random stiffness matrix, the random response vector and the random forcing vector respectively and superscript '*R*' denotes random.

Any random variable can be expressed as the sum of its mean and the zero mean random variable which is expressed as

Random variable $\left(RV^R\right)$=mean $\left(RV^d\right)$ + zero-mean random variable $\left(RV^r\right)$

The operating random variables in the present case are defined as [24-27]

$$b^R = b^d + b^r;\ K_i^R = K_i^d + K_i^r;\ q_i^R = q_i^d + q_i^r;\ F_i^{(R)} = F_i^{TH(d)} + F_i^{(r)} \qquad (25)$$

We can express the above relations in the form:

$$b^R = b^d + \in b^r;\ K_{ij}^R = K_{ij}^d + \in K_{ij}^r;\ q_i^R = q_i^d + \in q_i^r;\ F_i^{(R)} = F_i^d + \in F_i^{(r)} \qquad (26)$$

where $\in$ is a scaling parameter, and is small in magnitude. The superscript'd' and '*r*' denote the mean and zero mean random part. Consider a class of problems where the zero-mean random variation is very small as compared to its mean part system properties. Using the Taylor series expansion and neglecting the second and higher-order terms since first order approximation is sufficient to yield results with desired accuracy having low variability as is the case in most of the sensitive application [24-27, 31]. Substituting Eq. (26) in Eq. (24) we get:

$$\left[K_{ij}^d + \in K_{ij}^r\right]\left\{q_j^d + \in q_j^r\right\} = \left\{F_i^{(d)} + \in F_i^{(r)}\right\}; \qquad (27)$$

Equating the terms of same order, we obtain the zeroth order perturbation equation and first order perturbation equation as fallows [24-27].

Zeroth order perturbation equation $\left(\epsilon^0\right)$: $$\left[K_{ij}{}^{d}\right]\left\{q_j{}^{d}\right\}=\left\{F_i^{(d)}\right\} \quad (28)$$

First order perturbation equation $\left(\epsilon^1\right)$: $$\left[K_{ij}{}^{d}\right]\left\{q_j{}^{r}\right\}+\left[K_{ij}{}^{r}\right]\left\{q_j{}^{d}\right\}=\left\{F_i^{(r)}\right\} \quad (29)$$

Obviously, zeroth order Eq. (28) is the deterministic and gives the mean response. The first order Eq. (39) on other hand represents its random counterpart and solution of this equation provides the statistics of the nonlinear bending response, which can be solved using the probabilistic methods like perturbation technique, Monte Carlo simulation, Newman's expansion technique [37,38].

Using Taylor's series expansion the system matrix, the displacement vector and forced vector can be expressed as [25-27]

$$\left[K_{ij}{}^{r}\right]=\sum_l \frac{\partial K_{ij}{}^{d}}{\partial b_l{}^{R}} b_l{}^{r}\ ,\ \left[q_j{}^{r}\right]=\sum_l \frac{\partial q_j{}^{d}}{\partial b_l{}^{R}} b_l{}^{r}\ ,\ \left[F_i{}^{TH(r)}\right]=\sum_l \frac{\partial F_i^{TH(d)}}{\partial b_l{}^{R}} b_l{}^{r} \quad (30)$$

Substituting Eq. (30) in Eq. (29) and equating the coefficients of b_l^r. For each *l*, we get:

$$\left[K_{ij}{}^{d}\right]\left\{\frac{\partial q_j{}^{d}}{\partial b_l{}^{R}}\right\}+\left[\frac{\partial K_{ij}{}^{d}}{\partial b_l{}^{R}}\right]\left\{W^{d}\right\}=\left\{\frac{\partial F_i^{TH(d)}}{\partial b_l{}^{R}}\right\},\ l=1,2\ldots \quad (31)$$

Using Eq. (31) we can solve the only unknown $\left\{\frac{\partial W^{d}}{\partial b_l{}^{R}}\right\}$, for each *l*.

Using Eq. (26), the total deflection response and its variance can be written as [24-27]

$$q_j=q_j{}^{d}+\left\{\frac{\partial q_j{}^{d}}{\partial b_l^{r}}\right\}b_l^{r} \quad \text{and} \quad \text{var}\left(q_j\right)=E\left[\sum_l \frac{\partial q_j{}^{d}}{\partial b_l{}^{R}} b_l{}^{r}\right]^2 \quad (32)$$

Where E [ ] and var (.) are the expectation and variance respectively. The variance can further be written as [24-27]

$$\text{var}\left(q_j\right)=\sum_l^N\sum_l^N diag\left[\frac{\partial q_j{}^{d}}{\partial b_l{}^{R}}\left(\frac{\partial q_j{}^{d}}{\partial b_l{}^{R}}\right)^T\right]E\left(b_l{}^{r},b_l{}^{r}\right) \quad (33)$$

where, *N* is the number of variables and $E\left(b_l{}^{r},b_l{}^{r}\right)$ is determined from the autocorrelation function of the underlying stochastic field of *b*, which can be written as [24, 25]

$$E\left(b_l{}^{r},b_l{}^{r}\right)=[\sigma_b][\rho][\sigma_b] \quad (34)$$

$$\text{Where, } [\sigma_b]=\begin{bmatrix}\sigma_{b1} & \ldots & \ldots & 0\\ 0 & \sigma_{b2} & \ldots & 0\\ \ldots & \ldots & \ldots & \ldots\\ 0 & \ldots & \ldots & \sigma_{bm}\end{bmatrix} \text{ and } [\rho]=\begin{bmatrix}1 & \rho_{12} & \ldots & \rho_{1m}\\ \rho_{21} & 1 & \ldots & \rho_{2m}\\ \ldots & \ldots & .. & \ldots\\ \rho_{m1} & \rho_{m2} & \ldots & 1\end{bmatrix} \quad (35)$$

Where $[\sigma_b]$, $[\rho]$ and *m* are the standard deviation (SD) of random variables, the correlation coefficient matrix and number of random variables, respectively.

Substituting Eq. (34) in Eq. (33), we obtain as:

$$\text{var}\left(q_j\right)=\left(\frac{\partial q_j{}^{d}}{\partial b_l{}^{R}}\right)[\sigma_b][\rho][\sigma_b]\left(\frac{\partial q_j{}^{d}}{\partial b_l{}^{R}}\right)^T \quad (36)$$

Eq. (36) express the covariance of the deflection in terms of standard deviations (SD) of random variables b_i (i=1, 2,…, R) and correlation coefficients. It is evident from Eq.(36) that the response coefficient of variation obtained by using the first perturbation techniques exhibits linear variation with all random variables in material properties, expansion of the hygrothermal coefficients, lamina plate thickness and lateral loading.

5. Result and discussion

The second order statistics (mean & standard deviation) of the nonlinear transverse central deflection of laminated composite spherical shell with random system properties subjected to hygrothermo-mechanical loading with different boundary conditions, plate thickness ratios, aspect ratios, lateral pressure and environmental conditions are obtained through numerical examples.

A nine noded Lagrange isoparametric element with 63 DOFs per element for the present HSDT model with von Karman non linearity has been used for discretizing the laminate. Based on convergence study conducted, a (8*8) mesh has been used through out the study. The mean and standard deviation of the transverse nonlinear central deflection are obtained considering all the random material inputs variables, thermal expansion and hygrothermal contraction coefficients, lateral pressure and lamina plate thickness taking individual and/or combined as random variables. Being a linear nature of variation random variables as mentioned earlier and passing through the origin, the results are only presented by against standard deviation (SD) of system

property equal to 0.10. However, the obtained results reveals that the stochastic approach would be valid up to SD = 0.20 [20]. Moreover the presented results would be sufficient to extrapolate the results for other SD values keeping in mind the limitation of FOPT.

In order to show the accuracy and efficiency of present solution methodology mean and SD results are compared with those available in literatures and independent Monte Carlo simulation. The basic random system parameters such as E_1, E_2, G_{12}, G_{13}, G_{23}, α_{12}, α_1, α_2, h, Q and β_{22} are modelled as the basic random variables which are sequenced and denoted as

$b_1=E_1$, $b_2=E_2$, $b_3=G_{12}$, $b_4=G_{13}$, $b_5=G_{23}$, $b_6=v_{12}$, $b_7=\alpha_1$, $b_8=\alpha_2$, $b_9=h$, $b10=Q$ *and* $b_{11}=\beta_{22}$

The following non dimensionalized nonlinear transverse mean central deflection has been used in the present study for uniformly distributed and sinusoidal load are as

$$W_0 = \frac{w\left(\frac{a}{2},\frac{b}{2}\right)}{h} \quad \text{and} \quad W_0 = w\left(\frac{a}{2},\frac{b}{2}\right)\left(\frac{100E_2h^3}{b^4q_0}\right)$$

Where $w\left(\frac{a}{2},\frac{b}{2}\right)$ is the mean dimensionalized transverse central deflection of piezoelectric elastically supported laminated composite sandwich plate.

In the present study, the various combination of boundary support conditions used in analysis are SSSS, CCCC, CSCS, are given as;

1. **All edges are simply supported (SSSS):**

$$u = w = \theta_y = \psi_y = 0, at x = 0, a$$
$$v = w = \theta_x = \psi_x = 0, at y = 0, b$$

2. **All edges are Clamped (CCCC):**

$$v = w = \theta_y = \theta_x = \psi_y = \psi_x = 0, at x = 0, a$$
$$u = w = \theta_y = \theta_x = \psi_y = \psi_x = 0, at y = 0, b$$

3. **Two opposite edge are clamped and others two are simply supported (CSCS):**

$$u = v = w = \theta_y = \theta_x = \psi_y = \psi_x = 0, at\ x = 0\ and\ y = 0$$
$$v = w = \theta_y = \psi_y = 0, at\ x = a;\ u = w = \theta_x = \psi_x = 0, at\ y = 0, b$$

For the computational analysis, the following properties of composite material are considered to be temperature dependent on temperature and moisture. The material properties taken in analysis are at reference temperature 21^0 C and moisture concentration at 0% are given as [12]

E_{f1}=220 GPa, E_{f2}=13.79 GPa, E_m=3.45 GPa, G_{f1}=8.79 GPa, v_{f12}=0.2, v_m=0.35, α_{f1}=-0.99*10e^{-6} ^{0}/C, α_{f2}=-10.08*10e^{-6} ^{0}/C, α_m =72.0*10e^{-6} ^{0}/C, β_m=0.33, T_{g0}=216^{0}C.

The piezoelectric (5A) material layered at different positions of fiber layers are given as:

E_{11p} = 63.0 GPa, E_{22p} = 63.0 GPa, G_{12p} = G_{13p} = G_{23p}= 24.3 GPa, v_{12p} = 0.3, E_{11p} = 63 GPa,

Figure 5.1 shows the validation study of mean of linear and non-linear central deflection of square clamped laminated sandwich composite plate by varying load parameter. The present results using C^O finite element method are in good agreement with available literature of Putcha et al [1984].

Figure 5.2 shows the Convergence study for mean central deflection of a square laminated composite plate is examined by using 3 x 3, 4 x 4, 5 x 5, 6 x 6 and 7 x 7 mesh size of elements and plotted. As the number of mesh size increases, the mean central deflection decreases converges from 5 x 5 mesh size. Therefore, the total number of element equal to 25 is taken into consideration for the computation of further numerical results.

Figure 5.3 (a)-(b) shows the effect of foundation parameters and load parameters with random change in only foundation parameters {bi= (9, 10) =0.10} on the (a) mean and (b) COV of central deflection of square simply supported laminated [0/90/C/90/0] plate for Vf=0.6, a/h=100. As the foundation parameter increases, the central deflection decreases. The decrease of central deflection is highest for change in shear foundation. The effect of COV of central deflection is still highest for random change in shear foundation only. The effect of mean and COV are more severe for higher loads.

Figure 5.4 (a)-(b) shows the effect of cross-ply and angle-ply symmetric and anti-symmetric lamination scheme and load parameter with random change in all system parameters {bi= (1,…,7) =0.10} on the (a) mean and (b) COV of central deflection of square laminated [0/90/C/90/0] simply supported sandwich composite plate and Vf = 0.6, a/h=100, Q=50. Among the different lamination scheme, mean central deflection of symmetric cross-ply or angle-ply is higher than anti-symmetric, cross-ply and angle-ply plate while, COV on central deflection of symmetric angle plate is lower. As the load parameter increases, mean central deflection increases and COV decreases.

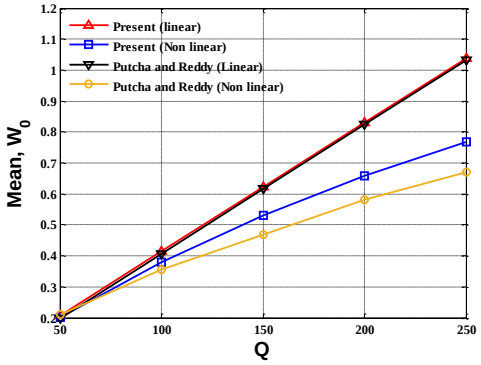

(a)

Figure 5.1 The validation study of mean of linear and non-linear central deflection of square clamped laminated sandwich composite plate by varying load parameter

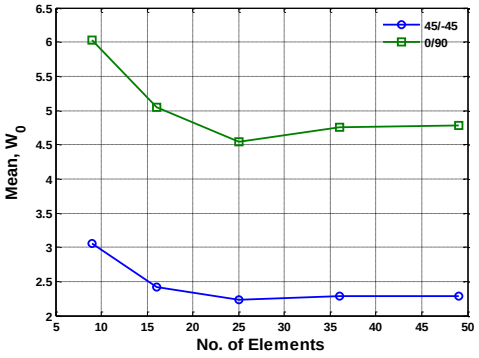

(b)

Figure 5.2 Convergence study for mean central deflection of a square laminated composite plate

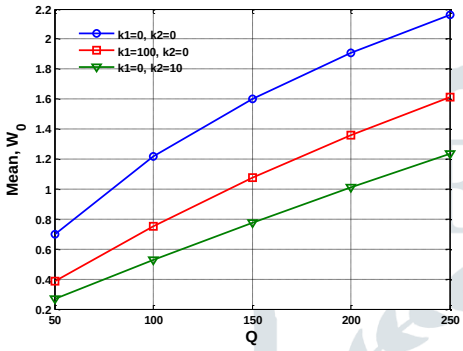

(a)

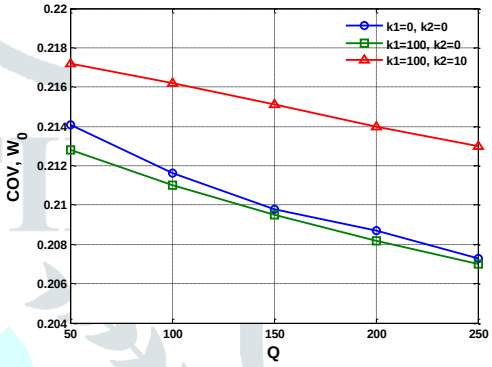

(b)

Figure 5.3 Effect of foundation parameters and load parameters with random change in only foundation parameters on the (a) mean and (b) COV of central deflection

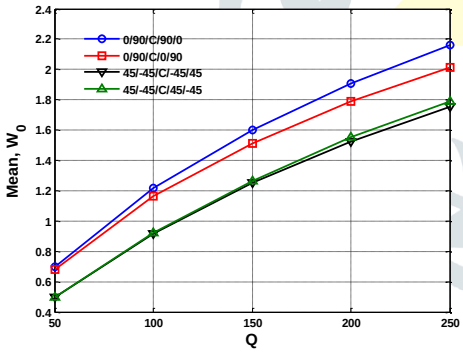

(a)

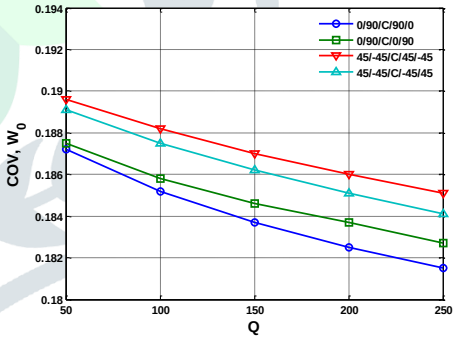

(b)

Figure 5.4 The effect of cross-ply and angle-ply symmetric and anti-symmetric lamination scheme and load parameter with random change in all system properties on the (a) mean and (b) COV of central deflection

Figure 5.5 (a)-(b) shows the effect of position of piezoelectric layer at various position of fiber layers and load parameter with random change in all system parameters {bi=(1,…,7) =0.10} on mean (a) and (b) COV of central deflection of simply supported square laminated composite plate for Vf=0.6, a/h=100. Among the given pizoelectric layer attached at different location of fiber layers, the mean central deflection is highest when piezo layer is attached at bottom place of fiber layer, However, COV of central deflection is highest when piezoelectric layer is attached at second position of fiber layer at Q=50, while, lowest when piezolayer attached with first position, at Q=50, COV of central deflection is highest when piezoelectric layer is attached at last position of fiber layer at Q=250, while, lowest when piezolayer attached with fourth position, at Q=250.

Figure 5.6 shows the effect of support conditions and load parameter with random change in all system parameters {bi=(1,…,7) =0.10} on the (a) mean and (b) COV of central deflection of square laminate [0/90/C/90/0] plate for Vf=0.5, a/h=100. Among the different support conditions, mean central deflection of clamped supported plate is lowest while, COV of simply supported plate is lowest. It is because of higher boundary constraits decreases the mean and increases the COV of central deflection. The change in mean of central deflection for Q=250 is highest, and COV of central deflection is highest at Q=50.

Figure 5.7 shows the effect of volume fraction of fibre, load parameter with random change in system parameters {bi=(1,…,7) =0.10} on the (a) mean and (b) COV of central deflection of simply supported square laminate [0/90/C/90/0] plate for Vf=0.6, a/h=100. As the fiber volume fraction increases, the mean central deflection decreases and COV of central deflection increases with increase of fiber volume fraction and effect are more pronounced when low volume of fiber with low load parameter is considered.

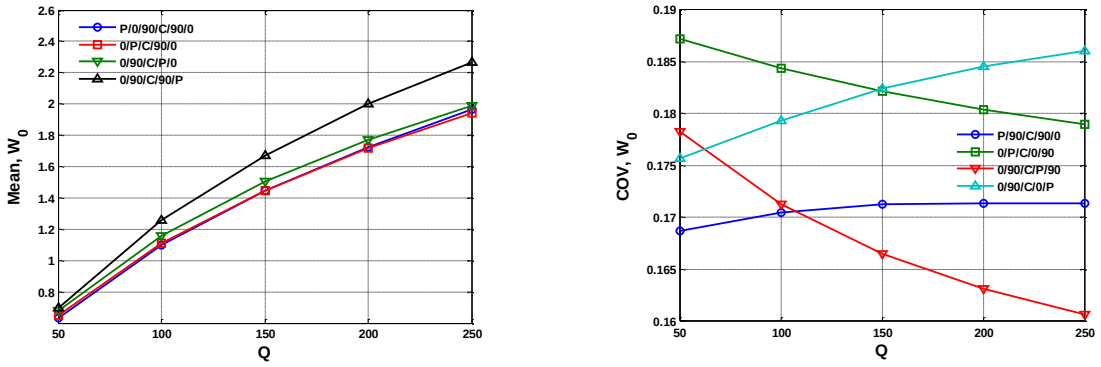

(a) (b)

Figure 5.5 Effect of position of piezoelectric layer at various position of fiber layers and load parameter with random change in all system parameters on mean (a) and (b) COV of central deflection

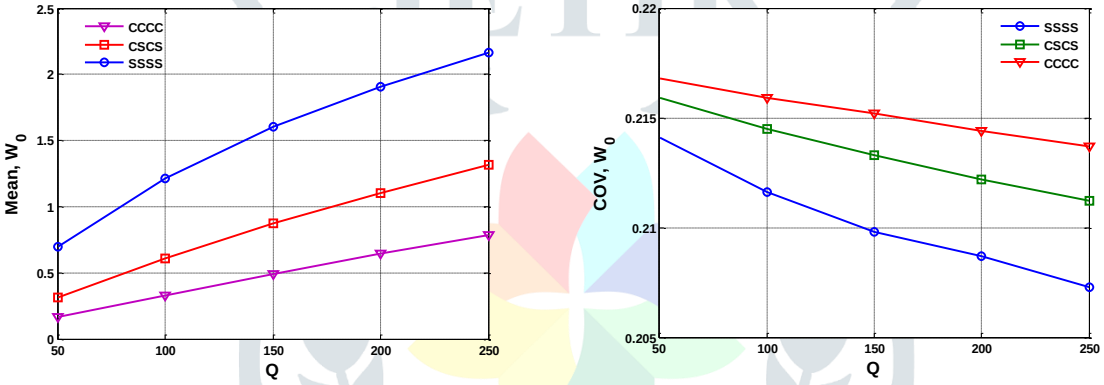

(a) (b)

Figure 5.6 Effect of support conditions and load parameter with random change in all system parameters on the (a) mean and (b) COV of central deflection of square laminate plate

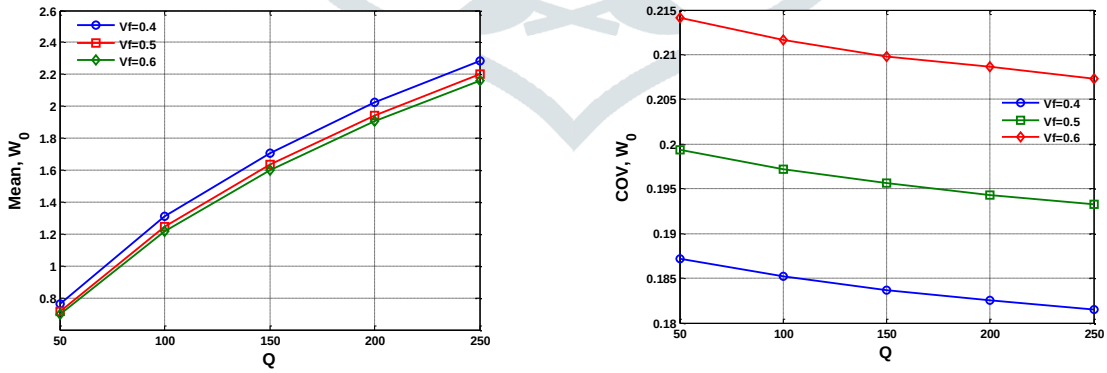

(a) (b)

Figure 5.7 Effect of volume fraction of fibre, load parameter with random change in system parameters on the (a) mean and (b) COV of central deflection

Figure 5.8 shows the effect of presence and absence of core sheet, load parameter with random change in system parameters {bi=(1,…,7) =0.10} on the (a) mean and (b) COV of central deflection of square laminate [0/90/C/90/0] plate for Vf=0.6, a/h=100, with clamped boundary condition at two opposite edge and simply supported at other two. Mean of central deflection increases as the core sheet is introduced between the face sheets and central deflection increases as load parameter increases. Also COV of laminates with core sheets is lower than that of the laminate without core, COV decreases as the load parameter increases.

Figure 5.9 shows the effect of temperature change, moisture change, volume fraction of fibre and load parameter with random change in system parameters {bi=(1,…,7) =0.10} on the (a) mean and (b) COV of central deflection of simply supported square

laminate [45/-45/45/-45] plate for Vf=0.6, a/h=10. The mean of central deflection increases as change in temperature, moisture and volume fraction decreases, but COV increases as change in temperature, moisture and volume fraction increases.

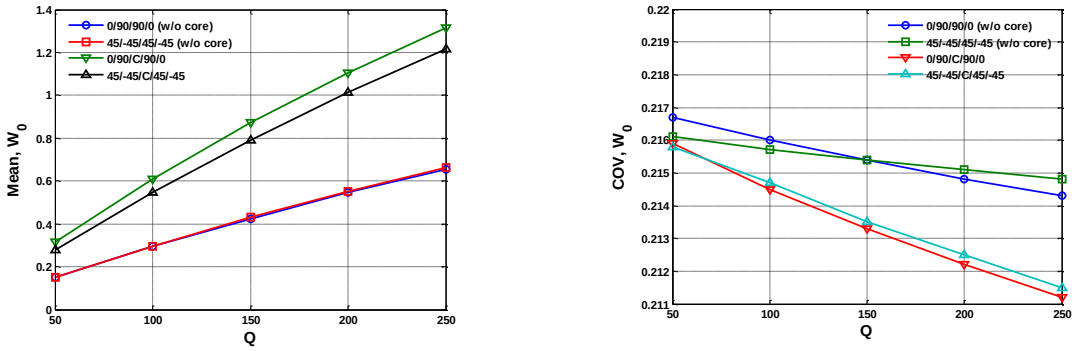

(a) (b)

Figure 5.8 Effect of presence and absence of core sheet, load parameter with random change in system parameters on the (a) mean and (b) COV of central deflection

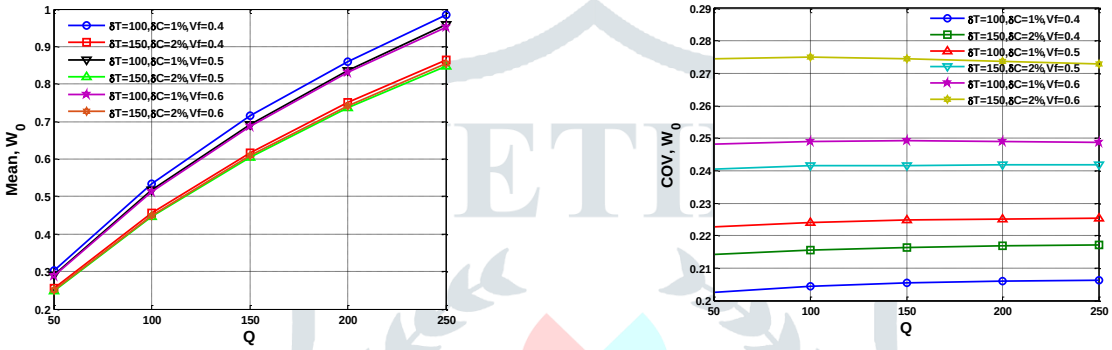

(a) (b)

Figure 5.9 Effect of temperature change, moisture change, volume fraction of fibre and load parameter with random change in system properties on the (a) mean and (b) COV of central deflection

Figure 5.10 shows the variation of central deflection along the length of the plate with different volume fraction and load parameters for simply supported square laminate [0/90/C/90/0], a/h=100. Mean of central deflection increases as x/a increases and is maximum at the centre of the plate and then decreases. As Vf decreases central deflection increases.

Figure 5.11 shows the validation study of COV of central deflection of square clamped laminated sandwich composite plate by varying load parameter {bi=(1,…,7) =0.10} using SOPT and MCS for clamped square laminated [0/90/C/90/0] plate with Vf=0.5, a/h=100. It shows good agreement of the present method with the MCS method.

Figure 5.12 shows the effect of COC of random change in system properties and load parameter with random change in all system parameters {bi=(1,…,7) =0.10}on the COV of central deflection for clamped square laminated [0/90/C/90/0] plate with Vf=0.5, a/h=100. As the COC increase COV of the central deflection increases.

Figure 5.13 shows the effect of load parameter and COC of random change in system properties with random change in only load parameter {bi=(14) =0.10} on the COV of central deflection for clamped square laminated [0/90/C/90/0] plate with Vf=0.5, a/h=100. As the COC increases COV increases linearly.

Figure 5.14 shows the comparison study with HSDT for mean central deflection of square laminated [0/90/C/90/0] plate with different load parameter and support condition. Figure shows good agreement with HSDT results.

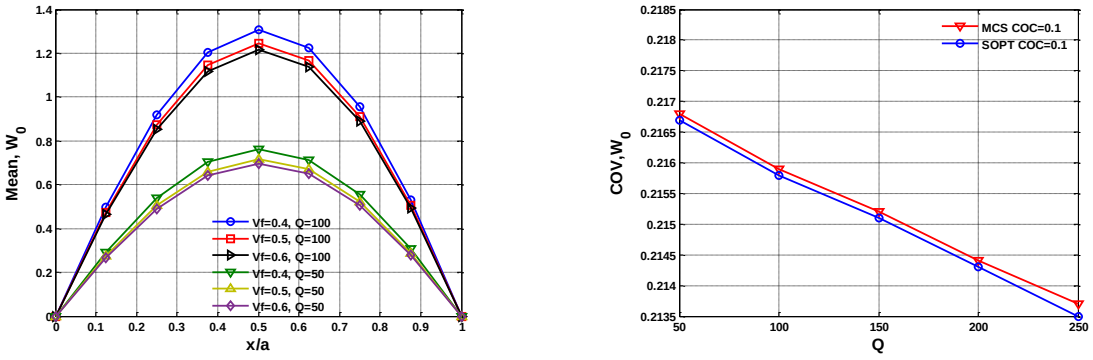

(a) (b)

Figure 5.10 Variation of central deflection along the length of the plate with different volume fraction and load parameters

Figure 5.11 The validation study of COV of central deflection of square clamped laminated sandwich composite plate by varying load parameter using SOPT and MCS

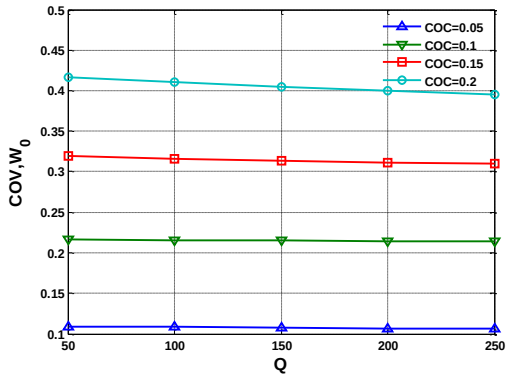

(a)

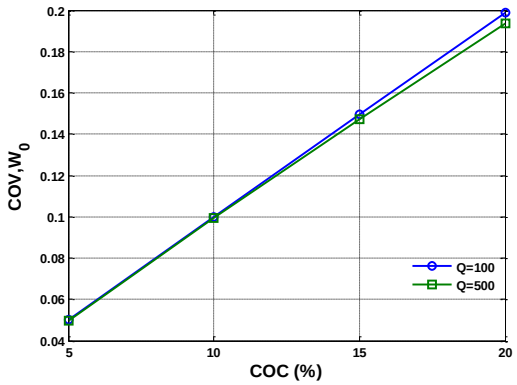

(b)

Figure 5.12 Effect of COC of random change in system properties and load parameter with random change in all system parameters on the COV of central deflection

Figure 5.13 Effect load parameter and COC of random change in system properties with random change in only load parameter on the COV of central deflection

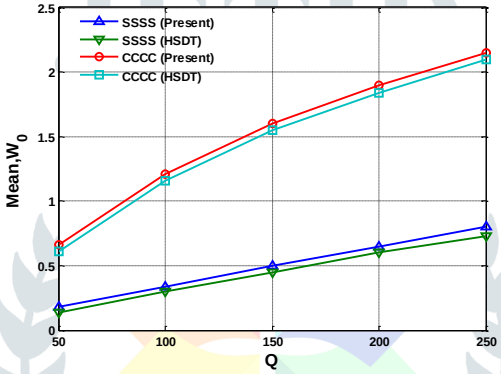

Figure 5.14 Comparison study with HSDT for mean central deflection of square sandwich composite plate with different load parameter

a/b=1, 45/-45/C/-45/45, SSSS, Vf=0.6

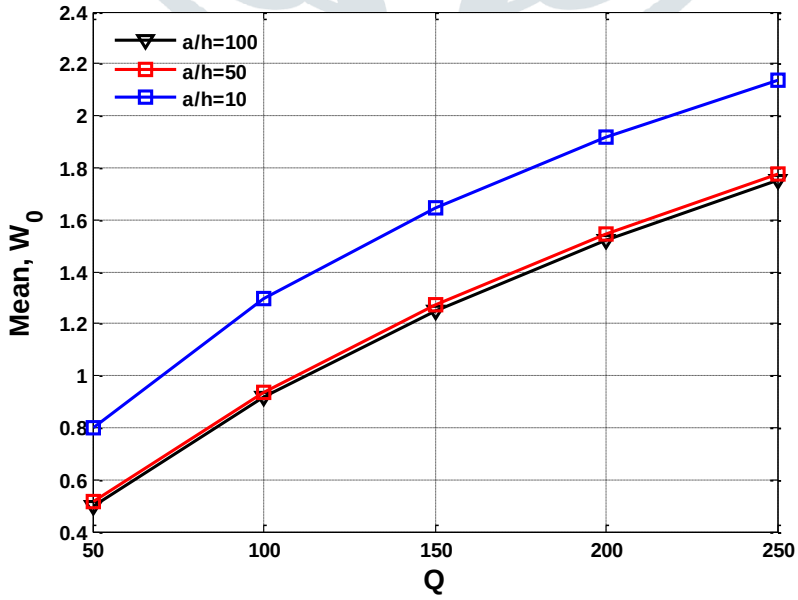

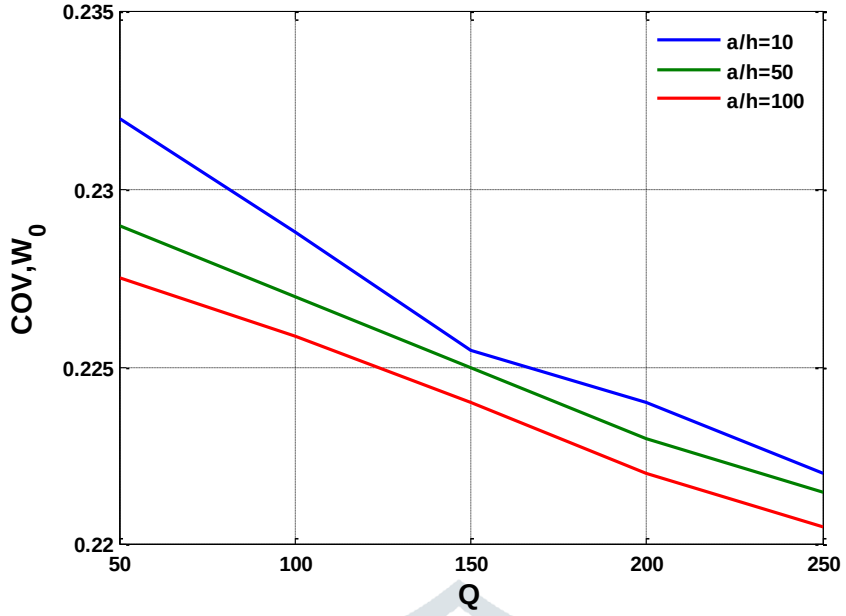

Figure 5.15

a/b=1,a/h=100, 45/-45/C/-45/45, SSSS, Q=50

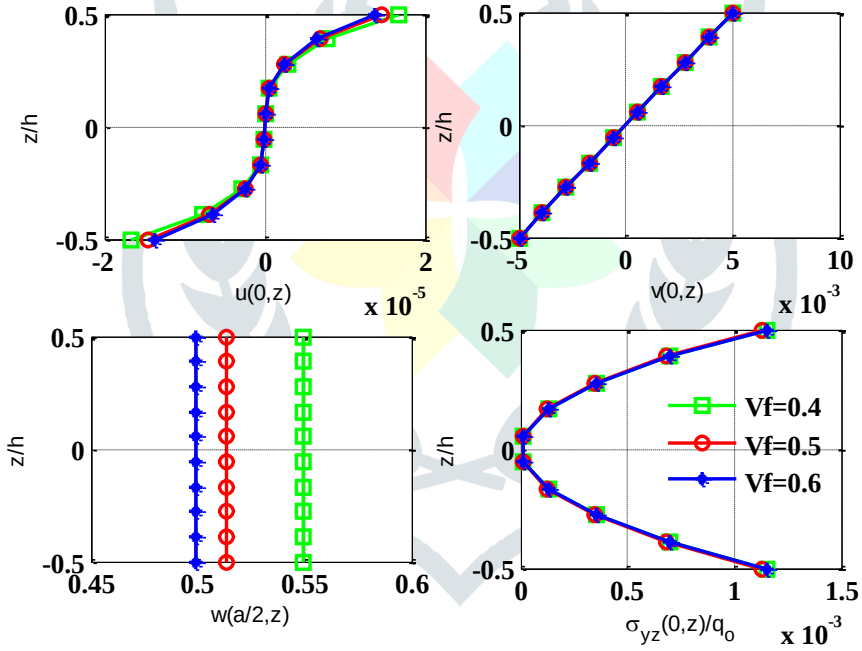

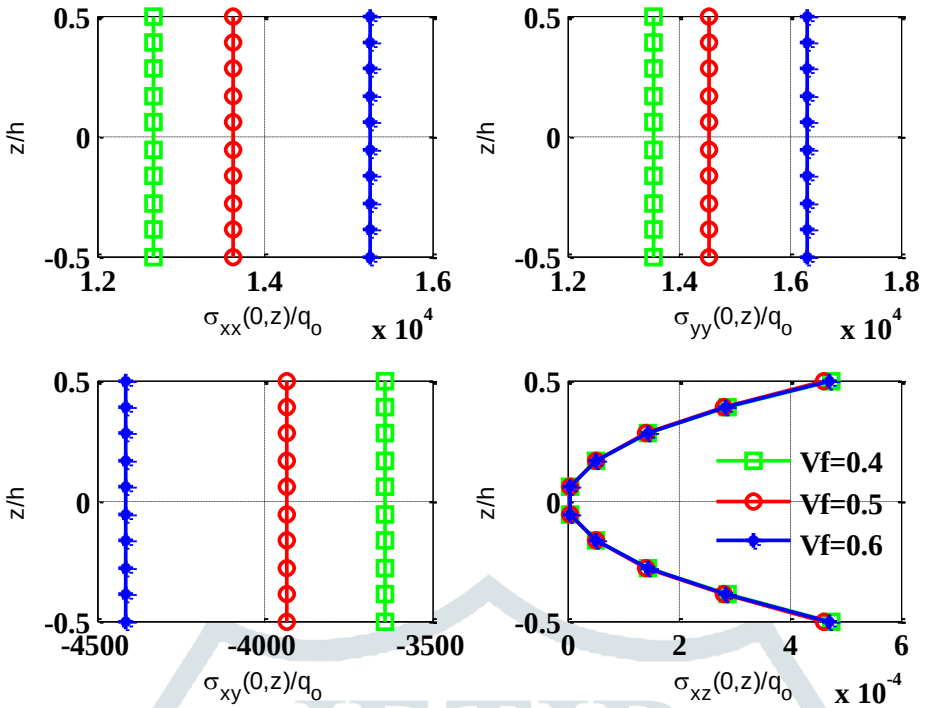

Figure 5.16

Table 5.1:- Flexural behaviour of three layered laminated plate [0/90/0] subjected to UDL.

Source	a/h					
	2	4	10	20	50	100
Simulated results	7.8525	2.9328	1.1287	0.7785	0.6842	0.6706
Sheikh and Chakrabarti (2003)	7.767	2.9093	1.091	0.7763	0.6841	0.6708
Reddy(1984)	7.767	2.9091	1.09	0.776	0.6838	0.6705
Ghosh and Dey (1990)	----	----	0.965	0.7572	----	0.6823

Table 5.2: Influence of boundary condition on non-dimensional deflection of anti-symmetric laminate [0/90] subjected to SSL.

Boundary condition	Source	W	
		a/h=5	a/h=10
SSSS	Simulated results (SFSDT)	1.62	1.2
	Reddy (HSDT)	1.6	1.2
SCSS	Simulated results (SFSDT)	1.3	0.81
	Reddy (HSDT)	1.23	0.8
SCSC	Simulated results (SFSDT)	1.3	0.6
	Reddy (HSDT)	1.1	0.56

4.3 Three layered sandwich plate subjected to uniform pressure

The flexural behaviour of a sandwich plate constituted of two orthotropic face sheets and one orthotropic core [0/C/0] with its all edges simply supported under the influence of uniform pressure is examined in terms of deflection and stresses at critical points. The ratio of core-thickness (h_c) to total thickness (h) of the plate is 0.8 while the thickness of each face-sheet (h_f) is 0.1 times the thickness of plate. The material properties of the orthotropic core are given.

$$[Q]_{core} = \begin{bmatrix} 0.999781 & 0.231192 & 0 & 0 & 0 \\ 0.231192 & 0.524886 & 0 & 0 & 0 \\ 0 & 0 & 0.26810 & 0 & 0 \\ 0 & 0 & 0 & 0.266810 & 0 \\ 0 & 0 & 0 & 0 & 0.159914 \end{bmatrix}$$

The parameter R is multiplied with the reduced stiffness coefficients of core to obtain the face sheets properties. The static analysis is performed for R= 5, 10, and 15 for the plate with a/h =10 and non-dimensional deflection and stresses as described in Eq. (19) are evaluated. Table 4.4 shows the comparison of the present results along with the established results. The comparison of the present results and the existing results with the exact solution reveals the superiority of the present theory. It is observed that the percentage difference of the present results from the exact solution (Srinivas, 1973) is 1.38% as compared to 3.03% of Pandya and Kant (1988), 2.26% of Touratier theory (Xiang et al, 2009), 1.83% of Karama's theory (Xiang et al, 2009), 1.88% of Ferreira et al. (2003), 1.66% of Mantari et al. (2012) and 1.32% of ZZ results presented by Sahoo and Singh (2013). Thus, with the similar or less computational cost, SFSDT evaluates more accurate and efficient results for the flexural behaviour of sandwich plates.

Table 5.3:- Simply supported sandwich plate [0/C/0] subjected to UDL.

Source	R		
	5	10	15
Simulated results	257.31	155.88	116.91
Exact (Srinivas, 1973)	258.97	159.38	121.72
Touratier (Xiang et al.,2009)	253.989	153.139	113.964
Karama (Xiang et al.,2009)	253.638	153.357	114.585
Ferreira et al. (2003)	257.11	154.658	114.644
Mantari et al. (2012)	256.706	155.498	115.919
Sahoo and Singh (2013)	258.4292	159.1948	121.56

Table 5.4 shows the effect of individual random system parameters {bi= (1,…,14) =0.10} and fibre volume fraction on the dimensionless mean and COV of central deflection of piezoelectric elastically simply supported laminated [0/90/C/90/0] square plate using SOPT for a/h=100. The effect of COV on central deflection with random change in volume fraction of fiber, Young's modulus of fiber and matrix, plate thickness, lamination angle and load parameter are very high. Therefore, it is concluded that for sensitive and safe applications like aerospace, nuclear and other related applications, tight control of these random system properties are required if high reliability of the plate is desired.

Table 5.5 shows the effect of individual random system parameters {bi=(1,…,14) =0.10} and fibre volume fraction on the dimensionless mean and COV of central deflection of piezoelectric elastically simply supported laminated [P/90C/90/0] square plate using SOPT for a/h=100, k1=100, k2=10. The effect of COV on central deflection with random change in volume fraction of fiber, Young's modulus of fiber and matrix, plate thickness, lamination angle and load parameter are very high. Therefore, it is concluded that for sensitive and safe applications like aerospace, nuclear and other related applications, tight control of these random system properties are required if high reliability of the plate is desired.

Table 5.4: Effects of individual random variable and fibre volume fraction on the dimensionless mean and COV of central deflection of laminated [0/90C/90/0] simply supported square plate

b_i	Q	COV, W_0					
		Vf=0.4		Vf=0.5		Vf=0.6	
		MEAN	COV	MEAN	COV	MEAN	COV
V_f	50	0.7574	0.1414	0.7108	0.1606	0.6897	0.1809
	100	1.3086	0.1404	1.2443	0.1595	1.2151	0.1796
Ef_1	50	0.7591	0.0845	0.7134	0.0857	0.6934	0.0862
	100	1.3067	0.0832	1.2424	0.0845	1.2130	0.0850
Ef2	50	0.7633	0.0239	0.7179	0.0327	0.6982	0.0426
	100	1.3104	0.0240	1.2469	0.0328	1.2186	0.0428
Em	50	0.7642	0.0889	0.7184	0.0786	0.6983	0.0674
	100	1.3141	0.0897	1.2491	0.0792	1.2195	0.0680
Gf12	50	0.7621	0.0013	0.7165	0.0018	0.6965	0.0024
	100	1.3085	0.0014	1.2445	0.0019	1.2156	0.0026
vf12	50	0.7622	0.0011	0.7166	0.0014	0.6966	0.0017
	100	1.3086	0.0011	1.2446	0.0014	1.2441	0.0017
h1	50	0.7583	0.0798	0.7128	0.0796	0.6928	0.0795
	100	1.3054	0.0823	1.2412	0.0820	1.2119	0.0818
theta	50	0.7657	0.031	0.7200	0.030	0.7000	0.028
	100	1.3075	0.062	1.2438	0.060	1.2154	0.058
k1	50	0.7622	0	0.7166	0	0.6966	0
	100	1.3086	0	1.2446	0	1.2441	0
k2	50	0.7622	0	0.7166	0	0.6966	0
	100	1.3086	0	1.2446	0	1.2441	0
E1p	50	0.7622	0	0.7166	0	0.6966	0
	100	1.3086	0	1.2446	0	1.2441	0
E2p	50	0.7622	0	0.7166	0	0.6966	0
	100	1.3086	0	1.2446	0	1.2441	0
G12p	50	0.7622	0	0.7622	0	0.7622	0
	100	1.3086	0	1.3086	0	1.3086	0
Q	50	0.7645	0.0995	0.7187	0.0996	0.6985	0.0996
	100	1.3152	0.0992	1.2506	0.0992	1.2215	0.0993

Table 5.5: Effects of individual random variable and fibre volume fraction on the dimensionless mean and COV of central deflection of laminated [P/90C/90/0] simply supported square elastically supported plate

b_i	Q	W_0					
		Vf=0.4		Vf=0.5		Vf=0.6	
		MEAN	COV	MEAN	COV	MEAN	COV
V_f	50	0.1932	0.1076	0.1927	0.1354	0.1939	0.1661
	100	0.3827	0.1077	0.3819	0.1354	0.3846	0.1659
E_{f1}	50	0.1942	0.0164	0.1942	0.0154	0.1961	0.0139
	100	0.3843	0.0169	0.3843	0.0159	0.3880	0.0146
Ef2	50	0.1943	0.0397	0.1943	0.0543	0.1961	0.0714
	100	0.3846	0.0396	0.3845	0.0542	0.3881	0.0712
Em	50	0.1933	0.1337	0.1936	0.1190	0.1957	0.1028
	100	0.3831	0.1332	0.3835	0.1186	0.3875	0.1024
Gf12	50	0.1943	1.8484e-04	0.1944	2.4566e-04	0.1963	3.2892e-04
	100	0.3845	1.7734e-04	0.3846	2.3903e-04	0.3883	3.2542e-04
vf12	50	0.1943	2.1749e-04	0.1944	2.5222e-04	0.1963	2.7405e-04
	100	0.3845	2.2420e-04	0.3846	2.6145e-04	0.3883	2.8618e-04
h1	50	0.1942	0.0227	0.1942	0.0223	0.1961	0.0213
	100	0.3842	0.0235	0.3842	0.0232	0.3880	0.0222
thetak	50	0.1948	4.6161e-04	0.1947	3.5596e-04	0.1966	2.3738e-04
	100	0.3853	0.0015	0.3853	0.0013	0.3890	0.0011
k1	50	0.1942	0.0244	0.1943	0.0245	0.1962	0.0249
	100	0.3844	0.0242	0.3844	0.0243	0.3881	0.0247
k2	50	0.1940	0.0476	0.1940	0.0477	0.1959	0.0483
	100	0.3839	0.0471	0.3839	0.0473	0.3876	0.0479
E1p	50	0.1943	0.0038	0.1943	0.0046	0.1963	0.0050
	100	0.3845	0.0035	0.3845	0.0043	0.3883	0.0046
E2p	50	0.1943	0.0015	0.1944	0.0013	0.1963	0.0011
	100	0.3845	0.0015	0.3846	0.0013	0.3883	0.0011

G12p	50	0.1943	3.4193e-05	0.1944	3.6867e-05	0.1963	4.3615e-05
	100	0.3845	3.5938e-05	0.3846	3.8617e-05	0.3883	4.5217e-05
Q	50	0.2062	0.0999	0.2026	0.0999	0.2010	0.0999
	100	0.4106	0.0998	0.4035	0.0998	0.4002	0.0998

Table 5.5 shows the effect of individual random system parameters $\{b_i\ (i=1,\ldots,14) =0.10\}$ and load parameters with fibre volume fraction on the dimensionless mean and COV of transverse central deflection of piezoelectric elastically supported laminated [P/90C/90/0] square simply supported plate using SOPT for a/h=100, and k_1=100, k_2=10. As the fibre volume fraction increases, the mean and corresponding COV of transverse central deflection increases with random change in V_f,

The effect of COV on transverse central deflection central deflection with random change in volume fraction of fiber, Young's modulus of fiber and matrix, plate thickness, lamination angle and load parameter are very high. Therefore, it is concluded that for sensitive and safe applications like aerospace, nuclear and other related applications, tight control of these random system properties are required if high reliability of the plate is desired.

6. Conclusion

A C0 nonlinear finite element method based on SFSDT with von-Karman nonlinearity in conjunction with SOPT has been presented to obtain the mean and COV of transverse central deflection of elastically supported piezoelectric laminated sandwich composite plate. The following conclusions can be drawn from this study:

1) The central deflection increases with increase the load parameter non linearly.

2) As the foundation parameter increases, the central deflection decreases. The decrease of central deflection is highest for change in shear foundation. The effect of COV of central deflection is still highest for random change in shear foundation only

3) Among the given piezoelectric layer attached at different location of fiber layers, the mean central deflection is highest when piezo layer is attached at bottom place of fiber layer, However, COV of central deflection is highest when piezoelectric layer is attached at second position of fiber layer at Q=50, while, lowest when piezolayer attached with first position, at Q=50, COV of central deflection is highest when piezoelectric layer is attached at last position of fiber layer at Q=250, while, lowest when piezolayer attached with fourth position, at Q=250.

4) Among the different support conditions, mean central deflection of clamped supported plate is lowest while, COV of simply supported plate is lowest.

5) As the fiber volume fraction increases, the mean central deflection decreases and COV of central deflection increases with increase of fiber volume fraction and effect are more pronounced when low volume of fiber with low load parameter is considered.

A direct iterative based stochastic finite element method (DISFEM) using higher order shear deformation plate theory [HSDT] and nonlinear von Karman kinematic have been used to obtain the second order statistics (mean and SD) of transverse nonlinear central deflection of composite plate with multiple randomness in material properties, thermal expansion coefficient, contraction coefficient, lateral loading and lamina plate thickness. The hygrothermal mechanical properties obtained by micromechanical model greatly affect the transverse central deflection of the laminated composite shell. Increase the temperature and moisture concentration, the dimensionless mean and SD of transverse nonlinear central deflection increases indicating that the shell becomes more sensitive with higher temperature and moisture content. The hygrothermal effects are more determinant as the working temperature increases and reaches closer to the glass transition temperature. Among the different random system properties studied, the longitudinal Young's modulus, mechanical loading and lamina thickness are most sensitive. The strict control of these parameters are therefore required if high reliability of the laminate composite shell is desired. The effect of volume fraction greatly influences the transverse central deflection of the shell. Increase the value of volume fraction mean transverse deflection and its SD decreases. It is due to the fact that with increase in fiber volume fraction, the stiffness of shell decreases. Clamped shell is most desirable in comparison with other support conditions for design point of view.

References

1. Reddy JN. Bending of laminated anisotropic shell by shear deformation finite element. Fibre Science Technology 1982;17: 9-24.
2. Reddy JN, Chao WC. Nonlinear bending of thick, rectangular laminated composite plate. International Journal Of Non Linear Mechanics 1981; 16: 291-301.
3. Zenkour AM. Analytical solution for bending of cross-ply laminated plates under thermo-mechanical loading. Composite Structures 2004; 65:367–379.
4. Panda SK, Singh BN. Nonlinear free vibration of spherical shell panel using higher order shear deformation theory – A finite element approach. International Journal of Pressure Vessels And Piping 2009; 86:373-83.
5. Chan HC, Chung WC. Geometrically nonlinear analysis of shallow shells using higher order finite elements. Composite Structures1989; 31(3):329–38.
6. Huang NN, Tauchert TR. Large deformation of antisymmetric angle-ply laminates resulting from non uniform temperature loadings. Journal of Thermal Stresses 1988;11:287-97.

7. Huang NN, Tauchert TR. Large deformation of laminated cylindrical and doubly-curved panels under thermal loading. Computers and Structures 1991;41(2): 303–12.
8. Chandrasekhara K, Bhimaraddi A. Thermal stress analysis of laminated doubly curved shells using a shear flexible finite element. Computers and Structures 1994; 52(5):1023–30.
9. Reddy JN, Chandrasekhara K. Nonlinear analysis of laminated shells including transverse shear strains. J. AIAA. 23(3), 440-441 (1985).
10. Ram KS, Sinha PK. Hygrothermal effects on the bending characteristics on laminated composite plates. Computers and Structures 1991;40(4):1009-15.
11. Shen HS. Hygrothermal effects on the nonlinear bending of shear deformable laminated plates. Journal of Engineering Mechanics 2002; 493-496.
12. Upadhyay AK, Pandey R, Shukla KK. Nonlinear Flexural response of laminated composite plates under hygro-thermo-mechanical loading. Communications in Nonlinear Science and Numerical Simulation 2010;15:2634-2650.
13. Zongeen Z, Suhaum C. The standard deviation of the eigensolution for random MDOF systems. Composite Structures 1990;39(6):603-607.
14. Naveenthraj B, Iyengar NGR, Yadav D. Response of composite plates with random material properties using FEM and MCS. Advanced Composite Material 1998;**7**:219-37.
15. Salim S, Yadav D, Iyengar NGR. Analysis of composite plates with random material characteristics. Mechanics Research communications1993;20(5): 405-14.
16. Onkar A K, Yadav D. Non-linear response statistics of composite laminates with random material properties under random loading.Composite Structures 2003; 60(4):375-83.
17. Yang J, Liew KM, Kitiponachi S. Stochastic analysis of compositionally graded plate with system randomness under static loading. International Journal of mechanical Science 2005;4:1519-1541.
18. Falsone G, Impollonia N. A new approach for the stochastic analysis of finite element modeled structures with uncertain parameters. Computer Methods in Applied Mechanics and Engineering 2002;191:5067-85.
19. Zhang Y, Chen S, Liu Q, Liu T. Stochastic perturbation finite elements. Composite Structures 1996;59(3): 425–429.
20. Liu W K, Ted B, Mani A. A random field finite elements. International Journal for Numerical Methods in Engineering 1986; 23:1831-1845.
21. Zhang J, Ellingwood B. Effects of uncertain material properties on structural stability. Journal of Structural Engineering 1993;121:705-716.
22. Noh HC. Effect of multiple uncertain material properties on the response variability of in-plane and plate structures.Computer Methods in Applied Mechanics and Engineering 2006;195:2697-2718.
23. Park JS, Kim CG, Hong C S. Stochastic finite element method for laminated composite structures.Journal of Reinforced Plastics and Composites 1995;14:675-93.
24. Lal A, Singh BN, Kumar R. Static response of laminated composite plates resting on elastic foundation with uncertain system properties. Journal of Reinforced Plastics and Composites 2007;26:807-29.
25. Singh BN, Lal A, Kumar R. Nonlinear bending response of laminated composite plates on nonlinear elastic foundation with uncertain system properties. Engineering Structures 2008;30:1101-1112.
26. Pandit MK, Singh BN, Sheikh AH. Stochastic perturbation-based finite element for deflection statistics of soft core sandwich plate with random material properties. International Journal of Mechanical Science 2009;51:363-371.
27. Lal A, Singh BN, Kumar R. Stochastic nonlinear bending response of laminated composite plates subjected to lateral pressure and thermal loading. Archive Appl. Mech. xx (2010);DOI 10.1007/s00419-010-0442-7 (Manuscript accepted).
28. Jones RM. Mechanics of composite materials. New York:McGraw-Hill;1975.
29. Agarwal BD, Laqrence,J B. Analysis and performance of fiber composites. New York: John Wiley & sons;1990.
30. Reddy JN. Energy and variational methods in applied mechanics. New York: Wiley;1981.
31. Kleiber M, Hien, TD. The stochastic finite element method. New York: Wiley; 1992.
32. Zang Z, Chen S. The standard deviations of the eigen solutions for random MDOF systems. Computers and Structures 1991;39(6):603-7.
33. Reddy JN. A simple higher-order theory for laminated composite plates. Journal of Applied Mechanics 1984;51:745-52.
34. SaiRam KS, SreedharBabu T. Study of bending of laminated composite shells. Part I: shells without a cut-out. Composite Structures 2001;51:103-116.
35. Stefanou G. The stochastic finite element method: Past, present and future. Computers Methods in Applied Mechanics and Engineering 2009;198:1031-1051.
36. Gibson RF. Principles of composite material mechanics. New York: McGraw-Hill Publications;1994.
37. Kaminski MM. Computational mechanics of composite materials. Sensitivity, Randomness and multis. Springer Verlag;2002.
38. Peng XQ, Geng L, Liyan W, Liu GR., Lam KY. A stochastic finite element method for fatigue reliability analysis of gear teeth subjected to bending. International Journal of Computational Mechanics 1998;21: 253-61.
39. Singh BN, Yadav D, Iyengar NGR. Free vibration of laminated spherical panels with random material properties. Journal of Sound and Vibration 2001;244(2):321-38.
40. Chamis, C. C., Sinclair, J.H.: Durability/life of fibre composite in hygro-thermal-mechanical environments. In: composite material: testing and design (sixth conference), ASTM, STP, **787**, 498-512, 1982.
41. Chamis, C. C.: Simplified composite micromechanics equation for mechanical, thermal and moisture related properties, engineers guide to composite materials, Materials Park, OH: ASM international; 1987.
42. Lee, S. M.: International encyclopaedia of composites-3.VCH publications; 1990.
43. Lee, S. M.: International encyclopaedia of composites-4.VCH publications; 1991.
44. Pengchang Shen, Peixiang He. Bending analysis of plates and spherical shells by multivariable spline element method based on generalized variational principle. Computers and Structures 1995; 55(1):151-157.

Figure Captions

1. Geometry of laminated composite spherical shell.
2. Schematic flow chart of stochastic nonlinear bending analysis.
3. Validation study of DISFEM and independent MCS the transverse nonlinear central deflection of laminated composite square angle-ply $[45^0/-45^0]_{2T}$ spherical shell.

Notations:

A_{ij}, B_{ij}, *etc:*	Laminate stiffness's
BB:	Strain-displacement matrix
a, b and h:	Shell length and breadth
b_i:	Basic random system properties
E_{11}, E_{22}:	Longitudinal and Transverse elastic moduli
G_{12}, G_{13}, G_{23}:	Shear moduli
h:	Thickness of the Shell
K^L, K^{NL}:	Linear and nonlinear bending stiffness matrix
$K^{(G)}$:	Thermal geometric stiffness matrix
NE, N:	Number of elements, number of layers in the laminated plate
NN:	Number of nodes per element
ϕ_i	Shape function of i^{th} node
Q:	Reduced elastic material constants
q:	Vector of unknown displacements, displacement vector of eth element
U,	Strain energy due to bending
u, v, w:	Displacements of a point on the mid plane of plate
$\left(\bar{u} \quad \bar{v} \quad \bar{w}\right)$:	Displacement of a point along $\left(x \quad y \quad z\right)$
{ }, { }:	Stress vector, Strain vector
ϕ_1 *and* ϕ_2:	Rotations of normal to mid plane about the ξ_1 *and* ξ_2 and axis respectively
$\left(\xi \quad \eta\right)$:	Cartesian coordinates
RVs:	Random variables
ΔT and ΔC:	Change in temperatures and moisture concentration

Aij, Bij, etc	:	Laminate stiffness's
a, b and h	:	Plate length, breadth and thickness
h	:	Thickness of the shell
ν_{12}	:	Poisson's ratio of cylindrical shell
b_i	:	Basic random variables
E_{11}, E_{22}	:	Longitudinal and Transverse elastic moduli
G_{12}, G_{13}, G_{23}	:	Shear moduli
K^L, K^{NL}	:	Linear and nonlinear plate stiffness matrix
K_g *and* K_m	:	Thermal and moiture geometric stiffness matrix
D	:	Elastic stiffness matrices
ne, n	:	Number of elements, number of layers in the laminated plate
$N_{\xi_1}^T\ N_{\xi_2}^T,\ N_{\xi_1\xi_2}^T$	:	In-plane thermal buckling loads
$N_{\xi_1}^V, N_{\xi_2}^V, N_{\xi_1\xi_2}^V$	:	In-plane electrical loads
E_k	:	The electric field vector
nn	:	Number of nodes per element
N_i	:	Shape function of ith node
D_k	:	The electric displacement vector
$\overline{C}^{\,p}{}_{ijkl}$	:	Reduced elastic material constants
$f, \{f\}^{(e)}$	:	Vector of unknown displacements, displacement vector of eth element
u, v, w	:	Displacements of a point on the mid plane of shell
$\overline{u}_1,\ \overline{u}_2,\ \overline{u}_3$	:	Displacement of a point $(\xi_1 \quad \xi_2 \quad \zeta)$
$\overline{\sigma}_{ij}, \overline{\varepsilon}_{ij}$	:	Stress vector, Strain vector
ξ_{kl}	:	The dielectric coefficient matrix
e_{kl}	:	The matrix of the piezoelectric coefficients
ϕ_1, ϕ_2	:	Rotations of normal to mid plane about the ξ_1 and ξ_2 axis respectively
$\theta_1, \theta_2, \theta_3$	:	Two slopes and angle of fiber orientation wrt ξ_1 - axis for kth layer
$(\xi_1 \quad \xi_2 \quad \zeta)$	:	Cartesian coordinates
V_k	:	Applied voltage across the kth ply
λ, *Var(.)*	:	Eigen value and variance
N_{crnl}	:	The dimensionalized post buckling load
λ_{crnl}	:	The nondimensionlized critical buckling load
RVs	:	Random variables
$\Delta T, \Delta C,$	:	Difference in temperatures and moistures
$\alpha_{11}, \alpha_{22}, \beta_{11}, \beta_{22}$	:	Thermal expansion and hygroscopic coefficients along ξ_1 and ξ_2 axis, respectively.

Appendix

$$[T]=\begin{bmatrix} 1 & 0 & 0 & z & 0 & 0 & g(z) & 0 & 0 & 0 & 0 & 0 & 0 \\ 0 & 1 & 0 & 0 & z & 0 & 0 & g(z) & 0 & 0 & 0 & 0 & 0 \\ 0 & 0 & 1 & 0 & 0 & z & 0 & 0 & g(z) & 0 & 0 & 0 & 0 \\ 0 & 0 & 0 & 0 & 0 & 0 & 0 & 0 & 0 & 1 & 0 & g'(z) & 0 \\ 0 & 0 & 0 & 0 & 0 & 0 & 0 & 0 & 0 & 0 & 1 & 0 & g'(z) \end{bmatrix}, \quad \text{(A.1)}$$

$$\text{Where, } g(z)=z\sec\left(\frac{rz}{h}\right)$$

$$\{\overline{\varepsilon_l}\}=\begin{Bmatrix} \varepsilon_1^0 \\ \varepsilon_2^0 \\ \varepsilon_6^0 \\ k_1^0 \\ k_2^0 \\ k_6^0 \\ k_1^2 \\ k_2^2 \\ k_6^2 \\ \varepsilon_4^0 \\ \varepsilon_5^0 \\ k_4^2 \\ k_5^2 \end{Bmatrix}=\begin{bmatrix} \partial/\partial x & 0 & 0 & 0 & 0 & 0 & 0 \\ 0 & \partial/\partial y & 0 & 0 & 0 & 0 & 0 \\ \partial/\partial y & \partial/\partial x & 0 & 0 & 0 & 0 & 0 \\ 0 & 0 & 0 & 0 & -\partial/\partial x & 0 & C1\partial/\partial x \\ 0 & 0 & 0 & -\partial/\partial y & 0 & C1\partial/\partial y & 0 \\ 0 & 0 & 0 & -\partial/\partial x & -\partial/\partial y & C1\partial/\partial x & C1\partial/\partial y \\ 0 & 0 & 0 & 0 & 0 & 0 & \partial/\partial x \\ 0 & 0 & 0 & 0 & 0 & \partial/\partial y & 0 \\ 0 & 0 & 0 & 0 & 0 & \partial/\partial x & \partial/\partial y \\ 0 & 0 & \partial/\partial y & -C2 & 0 & 0 & 0 \\ 0 & 0 & \partial/\partial x & 0 & -C2 & 0 & 0 \\ 0 & 0 & 0 & 0 & 0 & C2 & 0 \\ 0 & 0 & 0 & 0 & 0 & 0 & C2 \end{bmatrix}\begin{Bmatrix} u \\ v \\ w \\ \theta_y \\ \theta_x \\ \psi_y \\ \psi_x \end{Bmatrix} \quad \text{(A.2)}$$

Where $c_1=\dfrac{(\sec(\frac{r}{2}))}{(1+(\frac{r}{2})\tan(\frac{r}{2}))}$, and $c_2=1$

$$\left[T_\phi\right]=\begin{bmatrix} 1 & 0 & z & 0 & z^2 & 0 & 0 & 0 \\ 0 & 1 & 0 & z & 0 & z^2 & 0 & 0 \\ 0 & 0 & 0 & 0 & 0 & 0 & 1 & z \end{bmatrix}, \quad \text{(A.3)}$$

$$Q=\begin{bmatrix} \bar{Q}_{11} & \bar{Q}_{12} & \bar{Q}_{16} & 0 & 0 \\ \bar{Q}_{12} & \bar{Q}_{22} & \bar{Q}_{26} & 0 & 0 \\ \bar{Q}_{16} & \bar{Q}_{26} & \bar{Q}_{66} & 0 & 0 \\ 0 & 0 & 0 & \bar{Q}_{44} & \bar{Q}_{45} \\ 0 & 0 & 0 & \bar{Q}_{45} & \bar{Q}_{55} \end{bmatrix} \quad \text{(A.4)}$$

$$\bar{Q}_{11} = Q_{11}\cos^4\alpha + 2\left(Q_{12} + 2Q_{66}\right)\cos^2\alpha\sin^2\alpha + Q_{22}\sin^4\alpha$$
$$\bar{Q}_{12} = \bar{Q}_{21} = \left(Q_{11} + Q_{22} - 4Q_{66}\right)\cos^2\alpha\sin^2\alpha + Q_{12}\left(\cos^4\alpha + \sin^4\alpha\right)$$
$$\bar{Q}_{16} = \left(Q_{11} - Q_{12} - 2Q_{66}\right)\sin\alpha\cos^3\alpha + \left(Q_{12} - Q_{22} + 2Q_{66}\right)\sin^3\alpha\cos\alpha$$
$$\bar{Q}_{22} = Q_{11}\sin^4\alpha + 2\left(Q_{12} + 2Q_{66}\right)\cos^2\alpha\sin^2\alpha + Q_{22}\cos^4\alpha$$
$$\bar{Q}_{26} = \left(Q_{11} - Q_{12} - 2Q_{66}\right)\sin^3\alpha\cos\alpha + \left(Q_{12} - Q_{22} + 2Q_{66}\right)\sin\alpha\cos^3\alpha$$
$$\bar{Q}_{66} = \left(Q_{11} + Q_{22} - 2Q_{12} - 2Q_{66}\right)\cos^2\alpha\sin^2\alpha + Q_{66}\left(\cos^4\alpha + \sin^4\alpha\right)$$
$$\bar{Q}_{44} = Q_{44}\cos^2\alpha + Q_{55}\sin^2\alpha$$
$$\bar{Q}_{45} = \left(Q_{55} - Q_{44}\right)sin\alpha\cos\alpha - Q_{54}$$
$$\bar{Q}_{55} = Q_{55}\cos^2\alpha + Q_{44}\sin^2\alpha$$

with

$$Q_{11} = \frac{E_{11}}{\left(1-\nu_{12}\nu_{21}\right)}\ ,\ Q_{12} = \frac{\nu_{12}E_{22}}{\left(1-\nu_{12}\nu_{21}\right)} = \frac{\nu_{21}E_{11}}{\left(1-\nu_{12}\nu_{21}\right)} = Q_{21}\ ,$$
$$Q_{22} = \frac{E_{22}}{\left(1-\nu_{12}\nu_{21}\right)}\ ,\ Q_{66} = G_{12}\ ,\ Q_{44} = G_{13}\ , Q_{55} = G_{12}\ ,\ \nu_{21} = \frac{\nu_{12}E_{22}}{E_{11}}$$

$$\phi(x,y,z) = \phi^{(0)}(x,y) + z\phi^{(1)}(x,y) + z^2\phi^{(2)}(x,y). \tag{A.5}$$

$$[k] = \begin{bmatrix} k_{11} & k_{12} & 0 \\ k_{12} & k_{22} & 0 \\ 0 & 0 & k_{33} \end{bmatrix}. \tag{A.6}$$

$$D = \sum_{k=1}^{NL}\int_{z_{k-1}}^{z_k}[T]^T\left[\bar{Q}\right][T]dz = \begin{bmatrix} [A_1] & [B] & [E] & 0 & 0 \\ [B] & [C] & [F] & 0 & 0 \\ [E] & [F] & [H] & 0 & 0 \\ 0 & 0 & 0 & [A_2] & [M_2] \\ 0 & 0 & 0 & [M_2] & [N_2] \end{bmatrix} \tag{A.7a}$$

with

$$\left(A_{1_{ij}},\ B_{ij},\ C_{ij},\ E_{ij},\ F_{ij},\ H_{ij}\right) = \sum_{k=1}^{NL}\int_{z_{k-1}}^{z_k}\bar{Q}_{ij}^{(k)}\left(1,\ z,\ z^2,\ g(z),\ zg(z),\ g(z)^2\right)dz,$$

For i, j=1,2,6,

$$\left(A_{2ij}, M_{ij}, N_{ij}\right) = \sum_{k=1}^{NL}\int_{z_{k-1}}^{z_k}\bar{Q}_{ij}^{(k)}\left(1, g'(z), g'(z)^2\right)dz, \qquad \text{For } i, j=4, 5$$

$$[D_1] = \sum_{k=1}^{NL}\int_{z_{k-1}}^{z_k}[T]^T[e][T]dz = \begin{bmatrix} [0] & [0] & [0] & [M_1] & [N_1] \\ [0] & [0] & [0] & [N_1] & [P_1] \\ [0] & [0] & [0] & [Q_1] & [R_1] \\ [M_2] & [N_2] & [P_2] & [0] & [0] \\ [P_2] & [Q_2] & [R_2] & [0] & [0] \end{bmatrix}, \tag{A.7b}$$

with $\left(M_{1_{ij}},\ N_{1_{ij}},\ P_{1_{ij}},\ Q_{1_{ij}},\ R_{1_{ij}}\right) = \sum_{k=1}^{NL}\int_{z_{k-1}}^{z_k}e_{ij}^{(k)}\left(1,\ z,\ z^2,\ z^3,\ z^4\right)dz,$

where i=3, j=1,2,6,

$$\left(M_{2_{ij}},\ N_{2_{ij}},\ P_{2_{ij}},\ Q_{2_{ij}},\ R_{2_{ij}}\right) = \sum_{k=1}^{NL}\int_{z_{k-1}}^{z_k}e_{ij}^{(k)}\left(1,\ z,\ z^2,\ z^3,\ z^4\right)dz, \text{ where i=1,2, j=4,5,}$$

$$[D_2]=\sum_{k=1}^{NL}\int_{z_{k-1}}^{z_k}[T_\phi]^T[k][T_\phi]dz=\begin{bmatrix}[S_1] & [T_1] & [U_1] & [0] & [0]\\ [T_1] & [U_1] & [V] & [0] & [0]\\ [U_1] & [V] & [W] & [0] & [0]\\ [0] & [0] & [0] & [S_2] & [T_2]\\ [0] & [0] & [0] & [T_2] & [U_2]\end{bmatrix}, \quad \text{(A.7c)}$$

with

$$\left(S_{1_{ij}},\ T_{1_{ij}},\ U_{1_{ij}},\ V_{ij},\ W_{ij}\right)=\sum_{k=1}^{NL}\int_{z_{k-1}}^{z_k}k_{ij}^{(k)}\left(1,\ z,\ z^2,\ z^3,\ z^4\right)dz,$$

where i,j=1,2,

$$\left(S_{2_{ij}},\ T_{2_{ij}},\ U_{2_{ij}}\right)=\sum_{k=1}^{NL}\int_{z_{k-1}}^{z_k}k_{ij}^{(k)}\left(1,\ z,\ z^2\right)dz,$$

where i,j=3.

$$D_3=\begin{bmatrix}A_1 & 0\\ B & 0\\ E & 0\\ 0 & A_2\\ 0 & C_2\end{bmatrix},\quad D_4=\begin{bmatrix}A_1 & B & E & 0 & 0\\ 0 & 0 & 0 & A_2 & C_2\end{bmatrix},\quad D_5=\begin{bmatrix}A_1 & 0\\ 0 & A_2\end{bmatrix},$$

$$D_6=\begin{bmatrix}0 & 0 & 0 & M_1 & N_1\\ M_2 & N_2 & P_2 & 0 & 0\end{bmatrix}, \quad \text{(A.7)}$$

a/b=1,a/h=100, 45/-45/C/-45/45, SSSS, Q=50

$$D_7=\begin{bmatrix}0 & M_2\\ 0 & N_2\\ 0 & P_2\\ M_1 & 0\\ N_1 & 0\end{bmatrix},$$